Food Chemistry: X 21 (2024) 101235

Contents lists available at ScienceDirect

Food Chemistry: X

journal homepage: www.sciencedirect.com/journal/food-chemistry-x

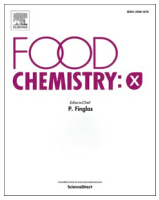

Advancements, limitations and challenges in hyperspectral imaging for comprehensive assessment of wheat quality: An up-to-date review

Yuling Wang [a,1], Xingqi Ou [a,1], Hong-Ju He [b,c,*,2,3], Mohammed Kamruzzaman [d,*,4,5]

[a] School of Life Science & Technology, Henan Institute of Science and Technology, Xinxiang 453003, China
[b] School of Food Science, Henan Institute of Science and Technology, Xinxiang 453003, China
[c] School of Chemistry, Chemical Engineering and Biotechnology, Nanyang Technological University, Singapore 637459, Singapore
[d] Department of Agricultural and Biological Engineering, University of Illinois at Urbana-Champaign, Urbana, IL 61801, USA

ARTICLE INFO

Keywords:
Wheat
Grain
Kernel
Hyperspectral imaging
Quality
Assessment

ABSTRACT

The potential of hyperspectral imaging technology (HIT) for the determination of physicochemical and nutritional components, evaluation of fungal/mycotoxins contamination, wheat varieties classification, identification of non-mildew-damaged wheat kernels, as well as detection of flour adulteration is comprehensively illustrated and reviewed. The latest findings (2018–2023) of HIT in wheat quality evaluation through internal and external attributes are compared and summarized in detail. The limitations and challenges of HIT to improve assessment accuracy are clearly described. Additionally, various practical recommendations and strategies for the potential application of HIT are highlighted. The future trends and prospects of HIT in evaluating wheat quality are also mentioned. In conclusion, HIT stands as a cutting-edge technology with immense potential for revolutionizing wheat quality evaluation. As advancements in HIT continue, it will play a pivotal role in shaping the future of wheat quality assessment and contributing to a more sustainable and efficient food supply chain.

1. Introduction

Wheat, originated and cultivated in the Middle East around 7000 BCE (Abdel-Aal et al., 1998), is arguably one of the most important and popular grain crops in the world, with highly indisputable importance (Igrejas & Branlard, 2020). Wheat is widely cultivated for its seeds and

Abbreviations: H-ELM, hierarchical extreme learning machine; SPA, successive projections algorithm; R_P^2, coefficient of determination of prediction; RMSEP, root mean square error of prediction; PCR, principal component regression; MLR, multiple linear regression; PLSR, partial least square regression; IVISSA, interval variable iterative space shrinkage approach; IRIV, iteratively retains informative variables; MASS, model adaptive space shrinkage; avNNet, averaging neural network; EWs, effective wavelengths; CAR, conditionally autoregressive; R, correlation coefficient; MSC, multiplicative scatter correction; SVM, support vector machine; MSE, mean squared error; RPD, ratio of performance deviation; S-G, Savitzky-Golay; SNV, standard normal variate; OSC, orthogonal signal correction; CFU, colony-forming unit; DON, deoxynivalenol; CNN, convolutional neural network; ASSDN, architecture self-search deep network; UVE, uninformative variable elimination; RFrog, random frog; SFLA, shuffled frog leaping algorithm; LPLS-S, local PLS based on global PLS scores; BPNN, back propagation neural network; GA, genetic algorithm; R_{CV}^2, coefficient of determination of cross-validation; RMSECV, root mean square error of cross-validation; LDA, linear discriminant analysis; FDK, Fusarium-damaged kernel; PCA, principal component analysis; RF, random forest; CARS, competitive adaptive reweighted sampling; SAE, sparse autoencoder; BPNN, backpropagation neural network; IVSO, iterative variable subset optimization; iCR, interval continuum removal; PLS-DA, partial least square discriminant analysis; SG2, Savitzky-Golay second derivative; ANN, artificial neural network; CNN-ATT, convolutional neural network with attention; CNN-FS, convolutional neural network based feature selector; ELM, extreme learning machine; DF, deep forest; LS-SVM, least square support vector machine; RMSEV, root mean square error of validation; gcForest, grained cascade forest; EMCVS, Monte Carlo variable selection; MSD, matched subspace detector; BPO, benzoyl peroxide; SAM, spectral angle mapping.

* Corresponding authors at: School of Food Science, Henan Institute of Science and Technology, Xinxiang 453003, China (H.-J. He).
E-mail addresses: hongju.he@hist.edu.cn (H.-J. He), mkamruz1@illinois.edu (M. Kamruzzaman).
[1] Contributed equally.
[2] ORCID: https://orcid.org/0000-0001-7112-5909.
[3] Scopus ID: 55515427300.
[4] ORCID: https://orcid.org/0000-0002-3525-3521.
[5] Researcher ID: O-2161-2013.

https://doi.org/10.1016/j.fochx.2024.101235
Received 8 December 2023; Received in revised form 7 February 2024; Accepted 15 February 2024
Available online 16 February 2024
2590-1575/© 2024 The Author(s). Published by Elsevier Ltd. This is an open access article under the CC BY-NC-ND license (http://creativecommons.org/licenses/by-nc-nd/4.0/).

belongs to the grass family Poaceae (Geren, 2021). The cultivation, processing, and distribution of wheat contribute significantly to the economies of many countries (Ahmed, Sulaiman, & Mohd, 2011). Besides, wheat is one of the most traded commodities on the global market, providing a significant portion of the world's food supply (Mitchell, & Mielke, 2005). Different varieties of wheat are cultivated to meet specific market demands, with the common wheat (*Triticum aestivum*) and durum wheat (*Triticum durum*) commonly used for food production (Rachon, & Szumilo, 2009). According to the statistics from the Food and Agriculture Organization of the United Nations (FAO), wheat is the third most produced grain crop around the world, after rice and maize. Its production is concentrated in over 80 countries, with the majority coming from a few countries in regions of Asia, Europe and the Americas (data from 2000 to 2021 shown in Fig. 1). China is currently the largest wheat producer globally, with an annual output over 100 million tons and a total production of 2.54 billion tonnes from 2000 to 2021, followed by India, Russia and the United States of America (FAO/FAOSTAT, 2021).

In the global food supply chain, wheat plays a vital and wide-ranging role, as it is not only a staple food to sustain human survival but also a good raw material to make a variety of food products, such as bread, pasta, noodles, cereals, cakes, pastries, and more (Cornell & Hoveling, 2020). Its versatility in processing makes it a fundamental ingredient in many cuisines worldwide. More importantly, wheat is a major source of dietary energy for a large portion of the world's population, providing valuable nutrients including carbohydrates, protein, fat, fiber, vitamins, essential amino acids, nucleic acids and minerals (Šramková, Gregová, & Šturdík, 2009), varying in different varieties and environmental conditions (Iqbal et al., 2015). Wheat-based products contribute significantly to the caloric intake of individuals globally (Hazard et al., 2020). In addition, with its sweet taste and good nature, wheat has sound effects of filling not only the stomach but also medical healing such as nourishing heart, strengthening spleen, nursing intestines, alleviating thirst, improving sleep, and so on (Shewry & Hey, 2015; Dinu et al., 2018).

Wheat quality is an extremely complex comprehensive concept (Troccoli et al., 2000), and can be divided into processing quality (e.g., primary processing quality such as grinding, flour yield, bulk weight, grain hardness, flour whiteness and ash content; secondary processing quality, also known as food production quality, such as flour quality, dough quality, baking quality, cooking rate, dough formation time, stability time, sedimentation value, softening degree, evaluation value, etc.) (Jayas et al., 2016; Pagani, Marti, & Bottega, 2014), edible quality (e.g. taste and flavor of products such as bread, noodles, cakes, pastries, etc. during baking, steaming and frying process) (Kucek et al., 2017), nutritional quality (mainly refer to the content of wheat nutrients) (Iqbal, Shams, & Fatima, 2022) and hygienic quality (e.g. toxic substances, harmful microorganisms, heavy metal pollution, pesticide residues, etc.) (Kovač et al., 2021), from different perspectives. There are both differences and correlations among these qualities (Knapp et al., 2017). One indicator can be used to reflect two or more qualities simultaneously (Schuster, Huen, & Scherf, 2023). Evaluating wheat quality involves considering factors such as protein content, gluten strength, moisture content, kernel size, hardness, color, impurities, and more (Varzakas, 2016). Wheat quality standards and specifications can vary across regions and countries, depending on the intended end-use of the wheat. Farmers, millers, and food processors closely monitor these quality characteristics to ensure that the wheat meets the requirements of the intended market and application. Quality assurance practices are essential throughout the entire production and supply chain to maintain high standards and consistency in wheat quality (Uthayakumaran, & Wrigley, 2017).

Wheat grain quality evaluation involves assessing various physical and chemical characteristics to determine its suitability for specific end-uses, which is generally performed using manual and chemical methods (Lasztity & Abonyi, 2009). These traditional methods cannot meet the requirement of on-site detection with a large amount of samples. It is, therefore, necessary and has been a trend to develop more advanced analysis tools, partially or completely replacing traditional detection methods, to evaluate wheat quality rapidly, non-destructive and accurately, improving detection efficiency and reducing costs. Optical techniques characterized by non-pretreatment, non-pollution, contactless, convenient and fast traits, such as near-infrared (NIR) spectroscopy (Du et al., 2022), and computer vision (CV) (Sabanci et al., 2017), have been investigated to evaluate wheat quality with good results. In principle, NIR is an electromagnetic wave in the 780–2526 nm range, dividing into two regions of NIR short wave (780–1100 nm) and NIR long wave (1100–2526 nm). NIR detection is mainly based on molecular vibration of double and harmonic absorption of hydrogen-containing group X–H (X = C, N, O) reflecting chemical compositions of a target sample. By mining NIR spectra, sample quality can be qualitatively analyzed to determine the compositions and structures of the substances or quantitatively evaluated to predict the contents of certain components in the substance or the values of substance quality attributes (Siesler et al., 2008). CV technique, a rapidly growing branch of artificial intelligence, uses computers to perform measurement and judgment, tasks traditionally done by the human eye. This technique converts the captured target into an image signal through CMOS or CCD camera, and transmits it to a dedicated image processing system to obtain morphological information, then converts it into a digital signal based on the pixel distribution, brightness, color and other information. Various image processing operations are carried out on these signals to extract

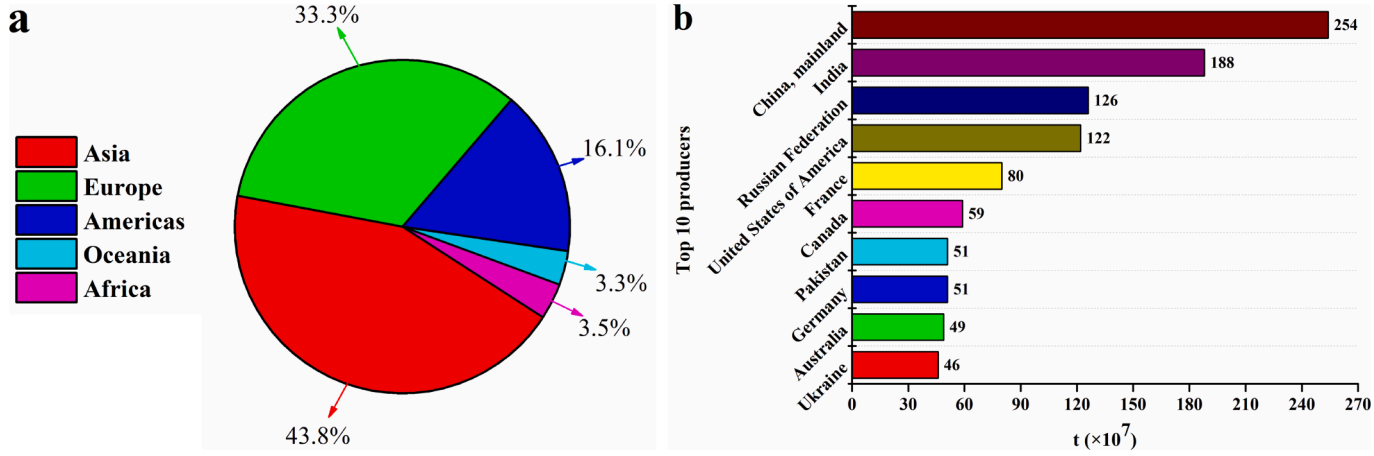

Fig.1. Statistics from FAOSTAT showing the distribution of total wheat production in 2000–2021, a. production share of wheat by region, b. top 10 producers.

characteristics of the target, such as area, quantity, position, length, and then output results according to preset tolerance and other conditions, including size, angle, number, qualified/unqualified, yes/no, etc., to achieve automatic recognition (Davies, 2017). Unlike the two optical techniques, hyperspectral imaging technology (HIT) provides not only spectral information indicating internal chemical composition information but also image information reflecting external morphological characteristics (He & Sun, 2015; Kamruzzaman, Makino, & Oshita, 2015). In other words, more information is offered by HIT and can be used to evaluate target quality more comprehensively and accurately, which is more advanced and beneficial than when NIR spectroscopy or CV are used alone. Unlike typical imaging systems that capture three bands (red, green, and blue), HIT captures data in numerous narrow and contiguous bands across the electromagnetic spectrum. Each pixel in a hyperspectral image contains a spectrum of information, allowing for detailed analysis and identification of materials based on their spectral signatures.

HIT has been applied and shows great potential in assessing wheat quality, providing a non-destructive and efficient way to assess multiple quality parameters simultaneously, and contributing to improved decision-making in wheat processing industries (An et al., 2023). To enhance and deepen the understanding of HIT in the quality evaluation of wheat, the research results on the use of HIT in evaluating wheat quality, in terms of physical, chemical and nutritional components determination, variety identification, fungal and mycotoxins detection, damage assessment, and adulteration classification, in the last five years (2018–2023) are comprehensively reviewed (shown as Fig. 2). The challenges of HIT in wheat quality evaluation and the prospects for its future industrial application are also discussed in this review.

2. HIT principle and analysis procedure

HIT system integrates imaging and spectroscopy techniques into one system to acquire spatial image information and spectral data, simultaneously. A typical HIT system consists of a spectrograph, camera, lighting device, moving platform and computer installed with data processing software, which are placed in a black box as shown in Fig. 3a.

HIT system produces three-dimensional (3-D) hypercubes (x, y, λ), including two-dimensional spatial data (λ) and one-dimensional spectral data (x, y), to form an image stack at continuous wavelengths, which can also be interpreted as stacking of spatial images (x, y) at different wavelengths (λ) (Fig. 3b). Hypercubes are typically obtained through three modes of light perception, such as reflection, transmission and interaction. The reflection mode is often used to assess external quality characteristics including color, size, surface texture, damages, and physical defects, while the transmission pattern is usually utilized to evaluate internal compositions and defects. More in-depth information can be obtained by interaction mode. The most appropriate mode can be selected to collect hypercubes based on the purpose of analysis and the nature of the sample. Four different patterns, including point-scanning, line-scanning, area-scanning and single-shot procedure, are used to acquire hyperspectral image, and line-scanning is the most commonly used pattern in food analysis.

Since a hypercube carries a large amount of data, several essential procedures are needed and executed to process the data by reducing data dimensions and redundant information. Four steps are generally required to process the hypercubes, including image acquisition and calibration, data extraction and processing, spectral data modeling, and spatial image generation (Fig. 3c). Among, a qualitative or a quantitative model is generally established to recognize or predict target index, and is commonly evaluated using correlation coefficient/coefficient of determination (R/R^2) and root-mean-square error (RMSE) in calibration set (R_C/R_C^2 & RMSEC), cross-validation set (R_{CV}/R_{CV}^2 & RMSECV) and prediction set (R_P/R_P^2 & RMSEP). Other parameters, including absolute value between $RMSE_C$ and $RMSE_P$, prediction bias, and residual predictive deviation (RPD), are also calculated to assess the model performance. Generally, a good model has higher R/R^2 and RPD values and lower RMSEC, RMSEP, and prediction bias values.

3. Application of HIT in wheat quality evaluation

3.1. Determination of chemical, physical and nutritional components

Wheat kernel contains various chemical components, some directly or indirectly affecting wheat quality. Specifically, moisture content directly influences the storage life and quality of wheat. Protein is one of the most important chemical components and nutrients in wheat and its level directly affects wheat gluten elasticity and taste. Starch is the main component of wheat, and its content directly affects the quality and taste of wheat gluten. Ash is a general term for inorganic substances in wheat, and its content is also one of the important indicators to evaluate wheat quality.

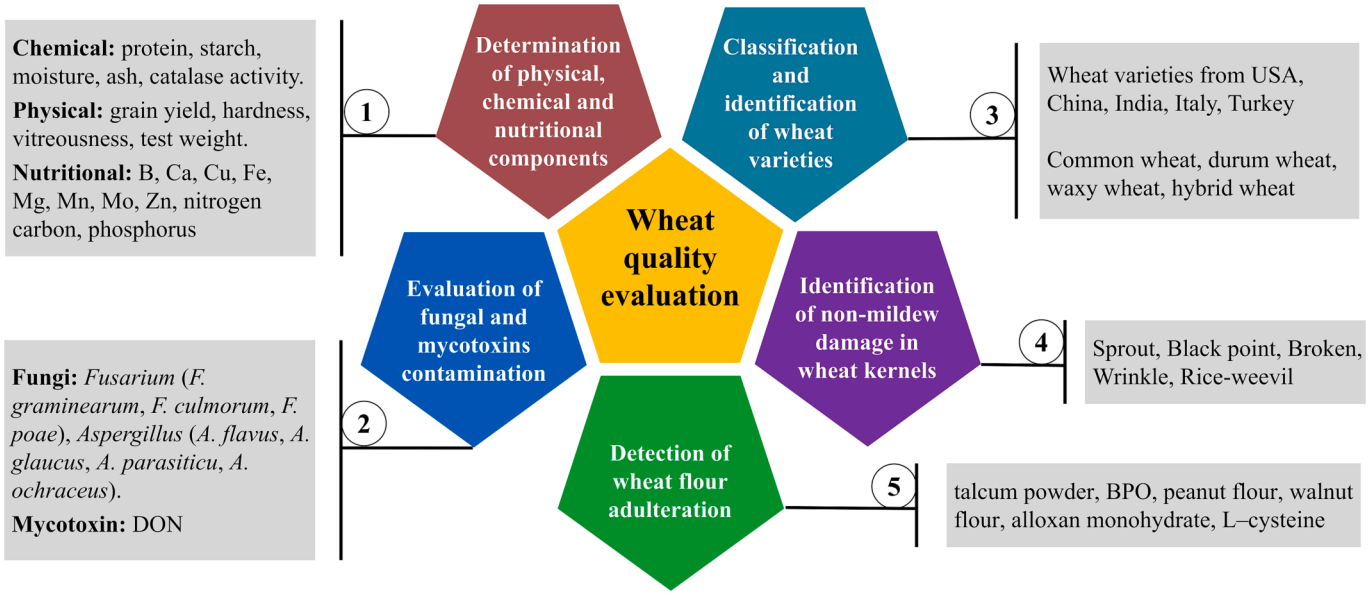

Fig. 2. Overview diagram of HIT for evaluating wheat quality in terms of several aspects using different indicators.

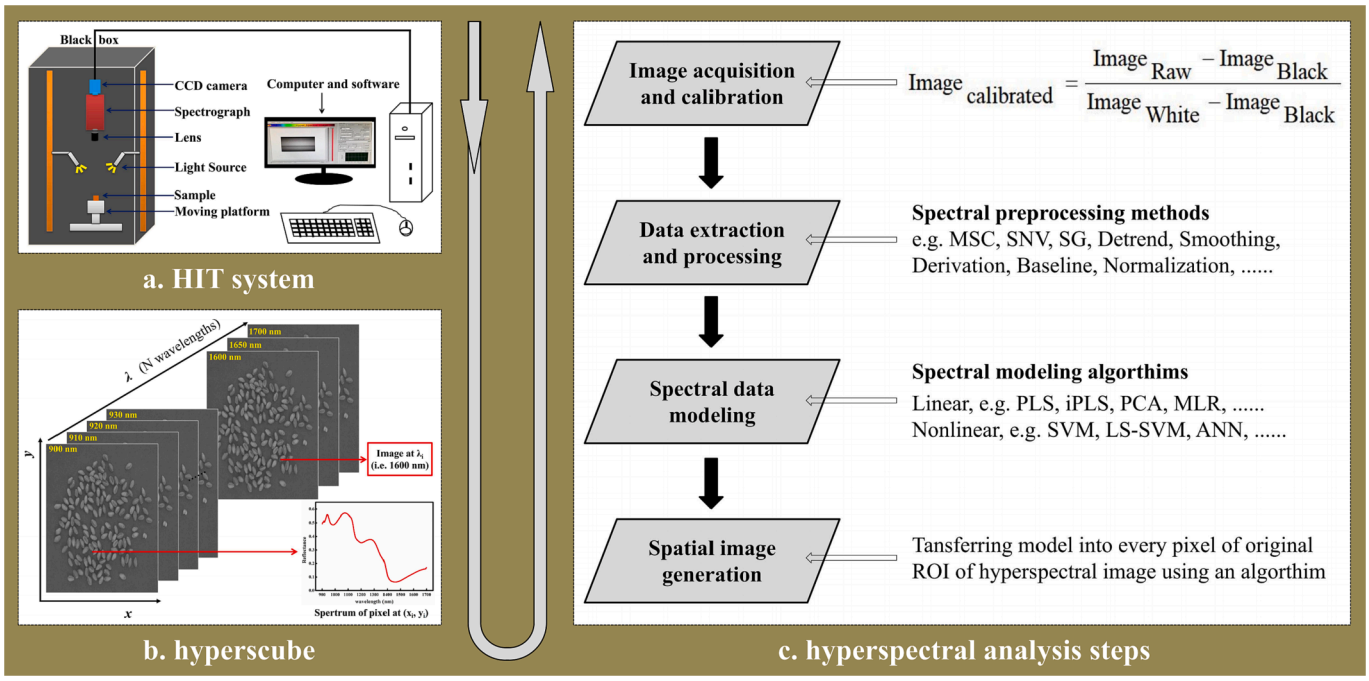

Fig. 3. General procedure of HIT for food quality analysis, a. HIT system, b. hyperscube, c. hyperspectral analysis steps.

In the recent five years, the concentration of these chemical components in wheat was predicted by HIT in different wavelength ranges combined with chemometrics. Caporaso et al. (2018) applied HIT in 980–2500 nm to determine protein distribution in whole single wheat kernels, obtaining prediction models with R_P^2 more than 0.8 and an error below 1 %, indicating an application potential in breeding wheat to select kernels based on their protein content. With two narrower spectral bands (1120–2424 nm, 969–2174 nm), excellent performance in predicting protein content in wheat flour was found by Morales-Sillero et al. (2018) (R_P^2 = 0.99, RMSEP = 0.21 %) and Zhang et al. (2023) (R_P^2 = 0.9859, RMSEP = 1.1580 g/100 g), respectively, which further highlighted the great potential of HIT in determining protein in a fast and non-destructive way. Moisture and starch contents of wheat flour were also measured and visualized by HIT using 28 and 52 effective wavelengths selected from the 969–2174 nm range, respectively, exhibiting a better effect of predicting starch ($R_P^2 > 0.9$) than predicting moisture ($R_P^2 < 0.9$)(Zhang et al., 2023). With 16 feature wavelengths selected from hyperspectral data (968–2576 nm) by successive projections algorithm (SPA), combined with Relieff-selected terahertz feature data, the ash content in wheat flour was well-predicted by a non-linear hierarchical extreme learning machine (H-ELM) model (R_P^2 = 0.989, RMSEP = 0.015 %) proposed by Li et al. (2023).

In addition to these common indicators, some uncommon indexes such as catalase activity, phosphorus, nitrogen, and carbon content can indicate wheat quality. Catalase activity is important for judging grain aging (Zhang et al., 2017). Eleven feature wavelengths were selected from 850 to 1700 nm range hyperspectral data to establish a high precision prediction model (R_P^2 = 0.9664), based on a support vector machine (SVM) algorithm, to quantify and visualize the catalase activity changes in wheat kernels very well (Zhang et al., 2022), which makes HIT a great potential to classify wheat based on the aging degree rapidly and non-destructively. Phosphorus is a key element related to cell wall and sugar content and is essential for wheat grain development. Phosphorus plays an important role in the effective growth, nutrient formation and grain quality of wheat. In the growth stage of wheat, a large amount of phosphorus is converted into constituent nutrients of wheat grain, thus promoting the growth of wheat in the later stage (Acevedo, Silva, & Silva, 2002). HIT in the 450–850 nm range was investigated to predict phosphorus content in the wheat kernel, but the results were not satisfactory (Pacheco-Gil et al., 2023). Nitrogen is very important in producing high yields and good wheat grain quality (Campillo, Jobet, & Undurraga, 2010). The carbon and nitrogen levels can affect the amounts and compositions of starch and protein in wheat, and thus affecting the wheat yield and quality traits (De Santis et al., 2021). Ground wheat samples were scanned and their nitrogen and carbon concentrations, as well as sample heterogenicity, were quantitatively well-predicted and vividly observed by applying HIT, with the combination of 1451–1600 nm, 1901–2050 nm and 2051–2200 nm most suitable for nitrogen prediction ($R_P^2 \geq 0.96$, RMSEP = 0.06 %), and 400–550 nm for carbon prediction (R_P^2 = 0.86, RMSEP = 0.21 %) (Tahmasbian et al., 2021).

Micronutrients such as B, Ca, Cu, Fe, Mg, Mn, Mo and Zn are important factors in assessing the nutritional quality of wheat (Njira & Nabwami, 2015). They are essential nutrients for human development (Welch & Graham, 2004). Micronutrients in wheat kernels and flour were measured by applying HIT, and the results indicated a better prediction of Ca, Mg, Mo, Zn in wheat kernels ($R_P^2 > 0.70$), and of Mg, Mo, Zn in wheat flour ($R_P^2 > 0.60$) (Hu et al., 2021).

Physical indexes, including grain yield, vitreousness, hardness, and test weight, are also used for wheat quality evaluation. High grain yield remains the top priority in wheat breeding and the major determinant factor for gaining economic benefit from producers (Zhang et al., 2021). Vitreousness is an important appearance marker for wheat grain hardness (Dexter et al., 1988). Hardness indicates wheat milling and end-use (Pasha, Anjum, & Morris, 2010). Test weight is used to reflect the bulk density of wheat grain (Wang & Fu, 2020). Among the four indexes, only the grain yield and hardness were well predicted by HIT ($R_P^2 > 0.80$), while the prediction of vitreousness and test weight by HIT was not satisfactory ($R_P^2 < 0.65$) (Erkinbaev, Derksen, & Paliwal, 2019; Vatter et al., 2022). Detailed information can be found in Table 1. Further study in developing an automatic removal of plot areas without vegetation covering may likely promote HIT's prediction accuracy.

Such wheat quality indexes can undergo dynamic changes throughout the various stages of wheat production, from cultivation to processing (Banach, Majewska, & Żuk-Gołaszewska, 2021; Filip et al., 2023). For example, proteins that contribute to the functional and

Table 1
Applications of HIT for assessing chemical, physical and nutritional components.

Sample	Target index	Wavelength range	Best spectral preprocessing method	Modeling algorithm	Selection method	Feature wavelengths (regions)	Best performance	Reference
Wheat flour	Ash	968–2576 nm	SNV	H-ELM	SPA	968.05, 1109.56, 1205.52, 1335.02, 1450.54, 1570.72, 1665.21, 1822.36, 1940.68, 1989.78, 2118.01, 2247.32, 2385.50, 2463.53, 2524.86, and 2530.44 nm	$R_P^2 = 0.989$ RMSEP = 0.015 %	Li et al., 2023
Wheat flour	Protein	969–2174 nm	None	Protein PCR	Protein IVISSA-IRIV	Protein 11 EWs selected by IVISSA-IRIV	Protein $R_P^2 = 0.9859$ RMSEP = 1.1580 g/100 g	Zhang et al., 2023
	Starch			Starch MLR	Starch IVISSA-IRIV	Starch 28 EWs selected by IVISSA-IRIV	Sarch $R_P^2 = 0.9243$ RMSEP = 0.2068 g/100 g	
	Moisture			Moisture PLSR	Moisture MASS	Moisture 52 EWs selected by MASS	Moisture $R_P^2 = 0.8646$ RMSEP = 2.1669 g/100 g	
Wheat kernel	Phosphorus	450–850 nm	None	CAR	Bayesian	500–690 nm	$R \geq 0.6$	Pacheco-Gil et al., 2023
Wheat kernel	Grain yield	410–990 nm	None	avNNet	None	None	Grain yield $R_P^2 = 0.84$ RMSEP = 0.94 Mg/ha	Vatter et al., 2022
	Protein						Protein $R_P^2 = 0.69$ RMSEP = 1.04 %	
	Vitreousness						Vitreousness $R_P^2 = 0.64$ RMSEP = 12.02 %	
	Test weight						Test weight $R_P^2 = 0.61$ RMSEP = 2.10 kg/hl	
Wheat kernel	Catalase activity	850–1700 nm	MSC	SVM	SPA	918.7, 956.2, 986.8, 1061.4, 1125.4, 1149.0, 1192.6, 1368.9, 1382.1, 1653.3, and 1672.7 nm	$R_P^2 = 0.9664$ MSE = 0.0064	Zhang et al., 2022
Wheat kernel	B, Ca, Cu, Fe, Mg, Mn, Mo, Zn	375–1050 nm	None	PLSR	None	None	Wheat kernel Ca, Mg, Mo, Zn $R_P^2 > 0.70$	Hu et al., 2021
Wheat flour							Wheat flour Mg, Mo, Zn $R_P^2 > 0.60$	
Wheat grain	Nitrogen	400–1000 nm	None	PLSR		Nitrogen 1451–1600 nm, 1901–2050 nm and 2051–2200 nm	Nitrogen $R_P^2 = 0.96$ to 0.99 RMSEP = 0.06 % RPD = 3.47–3.92	Tahmasbian et al., 2021
	Carbon	1000–2500 nm				Carbon 400–550 nm	Carbon $R_P^2 = 0.86$ RMSEP = 0.21 % RPD = 2.03	
Wheat kernel	Harderness	1000–2500 nm	S-G 1st derivative	ANN	None	None	$R_P^2 = 0.90$ RMSEP = 6.59	Erkinbaev et al., 2019
Wheat flour	Protein	1120–2424 nm	None	PLSR	None	None	$R_P^2 = 0.99$ RMSEP = 0.21 % RPD = 7.92	Sillero et al., 2018
Wheat kernel	Protein	980–2500 nm	SNV + 1st derivative	PLSR	None	None	$R_P^2 = 0.80$ RMSEP = 0.94 % RPD = 2.19	Caporaso et al., 2018

nutritional properties of wheat-based products can undergo aggregation during various stages, such as dough formation, baking, and storage (Abedi, & Pourmohammadi, 2021). Wheat protein aggregation is a complex process that significantly influences the functional properties of wheat-based products (Ortolan, & Steel, 2017). The interplay between gliadins and glutenins, along with external factors like hydration, mixing, and baking conditions, contributes to the formation of the gluten network and ultimately influences the quality of bread and other wheat-derived products (Ooms, & Delcour, 2019;Wieser, Koehler, & Scherf, 2023). HIT has not used to evaluate the impact of such biochemical

changes on wheat quality and should be the subject of in-depth study, potentially in combination with other techniques. By providing valuable insights into the biochemical pathways and compounds that influence wheat growth, development, and quality, metabolomics involving small molecules or metabolites within a biological system can be used as a powerful analytical approach for wheat quality analysis from a microscopic level (Saia et al., 2019; Păucean et al., 2021). Metabolomics and HIT are two distinct techniques and provide complementary information about different aspects of wheat samples. Metabolomics provides in-depth information about biochemical compositions, pathways, and concentrations of various metabolites, including sugars, amino acids, lipids, and organic acids (Tang et al., 2018; Razzaq et al., 2021), but cannot inherently provide spatial information on metabolite distribution within a sample. Understanding the metabolomic fingerprints of different wheat varieties contributes to breeding programs to improve quality traits (Litvinov, Karlov, & Divashuk, 2021). By integrating metabolomics and HIT, researchers and producers can better understand the factors influencing wheat quality. The combination of detailed biochemical information and spatial patterns enhances the precision of quality assessments, providing valuable insights for wheat management, breeding programs, and optimizing processing and production practices in the wheat industry.

3.2. Evaluation of fungal and mycotoxin contamination

Toxigenic molds can attack wheat grains during postharvest storage and processing. The mildew of wheat will affect the nutritional value and taste of grain and produce mycotoxins, which seriously threaten human health (Beccari et al., 2016). Mycotoxins are mainly toxic metabolites produced by mold in contaminated food; they can be delivered into human and animal bodies through feed or food, causing acute or chronic toxicosis, damaging the liver, kidney, nerve tissue, hematopoietic tissue and skin tissue (da Rocha et al., 2014). Rapid and visual detection of wheat mildew significantly reduces wheat storage losses. Early detection of mold infection degree is more important to control the mildew hazards. HIT has been proposed and used as an advanced optical technology for non-invasive and non-destructive detection, quantification, identification and discrimination of fungal and mycotoxins infections in wheat grains and flour.

Fusarium head blight (FHB) is one of the common diseases in wheat and wheat infected with FHB always has negative quality effects, such as grain atrophy, yield reduction, quality deterioration, and commodity value degradation, which cannot be neglected in the control of wheat quality (Hershman, Shaner, & Van Sanford, 2012). On the contrary, the prevention and control of FHB should be the top priority of the current wheat cultivation and production. Hyperspectral images of wheat kernels and flour infected with three *Fusarium* species (*F. graminearum*, *F. culmorum*, and *F. poae*) in 400–1000 nm and 1000–2500 nm ranges were investigated to reveal the different correlation between spectra and this fungal DNA (Alisaac et al., 2019). With HIT in the range of 400–1000 nm, 12 optimal wavelengths were selected and combined with corresponding images to identify *Fusarium*-damaged wheat kernels by random forest (RF) algorithm, generating an accuracy of classification up to 96.44 % (Zhang et al., 2020), almost the same as that of study performed by Delwiche et al. (2019), higher than that of other three studies (classification accuracy < 90 %) (Nadimi et al., 2021; Femenias et al., 2021a; Femenias et al., 2022), similar good as that by Ropelewska & Zapotoczny (2018) (accuracy, 85–98 %) and Delwiche et al. (2021) (accuracy, 70–96 %), but lower than that from Femenias et al., (2021b) (accuracy > 98.4 %) and Lv et al. (2022) (accuracy, 98.31 %), which is probably due to the different spectra, preprocessing, and chemometrics involved in analysis. Based on previous studies, Liu et al., (2022) attempted to use a multispectal imaging system carrying 19 wavelengths to monitor the *F. graminearum* growth in wheat kernels. The count of *F. graminearum* was predicted by a non-linear model (GA-SVM) with a correlation over 0.90, and the wheat kernels contaminated with *F. graminearum* was identified by a GA-BPNN model with an accuracy of 100 %. Besides *Fusarium*, another mold, namely *Aspergillus*, also easily causes wheat mildew (Mohapatra et al., 2017). The growth time of four *Aspergillus* including *A. flavus*, *A. glaucus*, *A. parasiticu*, and *A. ochraceus* in wheat grains was respectively quantified and distinguished by HIT using different number of characteristic wavelengths (13–17) with good performance (R_P^2, 0.882–0.932; RMSEP, 0.682–0.895) (Sun et al., 2023), which enables HIT to inspect the mold growth in wheat grains at early stage.

Deoxynivalenol (DON), a secondary metabolite produced by *Fusarium* strain, is the most important global mycotoxin in moldy wheat grains (Yuen, & Schoneweis, 2007). DON is an important indicator toxin of wheat grain mildew and is usually found in high concentrations in grain crops such as wheat, corn, barley, and oats (Van Der Fels-Klerx et al., 2012). DON is highly toxic to both humans and animals and has teratogenic, neurotoxic, embryonal toxic and immunosuppressive effects (Cimbalo et al., 2020). At present, the common methods used for detecting DON include mass spectrometry (MS), high-performance liquid chromatography (HPLC), electrochemical method, immunological method and so on (Ran et al., 2013). Although these methods are highly accurate and reliable, but often high-cost, time- and labor-consuming. HIT, representing a green and environmentally friendly emerging technology, was proposed to predict DON levels in FHB-infected wheat kernels rapidly and non-destructively. Based on 12 selected feature wavelengths, a SVM model was built to achieve a classification accuracy of 97.92 % for the testing set, and a visualization map was created to exhibit DON content (Liang et al., 2018). A feature range of 430–600 nm gave a classification accuracy of 100 % for wheat kernels and 96 % for wheat flour was obtained in the same research group (Liang et al., 2020), according to DON levels. Similar good results were also found in the other two studies conducted by Zhao et al. (2020) (96.92 %) and Shi et al. (2020) (94.29 %), respectively. By comparison, a classification accuracy below 90 % was reported by Femenias et al. (2020), Nadimi et al. (2021), Femenias et al. (2021a), and Femenias et al. (2022) (shown in Table 2). As for DON quantification by HIT, Shi et al. (2020) achieved the highest prediction accuracy (R_P, 0.9988; RMSEP, 365.3 μg/kg), better than other studies (Zhao et al., 2020; Femenias et al., 2020; Femenias et al., 2021a; Femenias et al., 2021b; Femenias et al., 2022; Shen et al., 2022; Dhakal et al., 2023). The reasons for the differences in the results among these studies may be related to wheat variety, spectral wavelength, wavelength preprocessing, modeling algorithm, and so on.

Overall, all these findings show that HIT is great potential and can be used to not only identify and classify wheat kernels contaminated with different levels of fungi but also detect mycotoxin content in wheat grains with good accuracy. Increasing spectral resolution of HIT to capture finer details in the unique spectral signatures associated with fungal contamination and mycotoxins will allow for more precise identification and characterization of specific contaminants. Coupled with advanced algorithms, including machine learning approaches (Zhang et al., 2022), the accuracy and reliability of contamination detection using HIT can be improved. Enhancing the sensitivity and selectivity of HIT for detecting low levels of fungal contamination and mycotoxins is crucial for early detection and prevention of mycotoxin-related issues in food and agricultural products. Though the integration of HIT with other detection technologies, such as molecular assays or biosensors (Wang et al., 2022; Oliveira et al., 2019), and the combination of complementary information provided by multiple techniques, the overall detection capabilities can be improved to a great extent. At present, it is still difficult to use HIT technology to identify and quantify a variety of toxins simultaneously, and future research on intelligent detection to make up for the shortcomings of HIT is expected.

3.3. Classification and identification of wheat varieties

Wheat varieties vary according to various factors such as origin,

Table 2
Applications of HIT for evaluating fungal and mycotoxins contamination.

Sample	Target index	Wavelength range	Best spectral preprocessing method	Modeling algorithm	Selection method	Feature wavelengths (regions)	Best performance	Reference
Wheat grain	Aspergillus flavus	400–1000 nm	OSC	SVM	SPA	Aspergillus flavus 401,467,595,719,868,931,945,950,954,955,956,957, 958 nm	R_P^2 = 0.834 RMSEP = 1.075 Log CFU	Sun et al., 2023
	Aspergillus glaucus					Aspergillus glaucus 424,430,434,438,439,444,476,570,622,671,706,788,888,911,916,920,921, 928 nm	R_P^2 = 0.822 RMSEP = 1.112 Log CFU	
	Aspergillus parasiticu					Aspergillus parasiticu 426,428,430,436,445,447,448,451,452,454,462,681, 709 nm	R_P^2 = 0.888 RMSEP = 0.871 Log CFU	
	Aspergillus ochraceus					Aspergillus ochraceus 434,441,443,447,452,454,458,465,493,530,569,601,699,847,905,915, 932 nm	R_P^2 = 0.832 RMSEP = 1.063 Log CFU	
	Fusarium graminearum					Fusarium graminearum 401,475,621,740,929,952,965,972,974,975,976,977,978,981, 983 nm	R_P^2 = 0.884 RMSEP = 0.882 Log CFU	
Wheat kernel	DON Fusarium	400–1000 nm	None	Mask R-CNN (prediction) G-Boost (classification)	None	None	R_P^2 = 0.75 Classification accuracy of 97 %	Dhakal et al., 2023
Wheat kernel	Fusarium	400–1000 nm	None	ASSDN	Combination of Relieff, UVE, RFrog, SFLA	941, 876, 732 nm	Classification accuracy of 98.31 %	Lv et al., 2022
Wheat kernel	DON	900–1700 nm	MSC SG smoothing	LPLS-S	None	None	R_P^2 = 0.81 RMSEP = 40.25 mg/kg RPD = 2.24	Shen et al., 2022
Wheat kernel	DON Fusarium	895–1728 nm	SNV	PLSR	Regression coefficients	1067,1159,1193,1222,1252,1343,1363,1378,1399,1497, and 1554 nm.	DON R_P^2 = 0.88 RMSEP = 6.66 mg/kg RPD = 3.21 Classification accuracy of 86 %	Femenias et al., 2022
Wheat kernel	Fusarium graminearum	405, 435, 450, 470, 505, 525, 570, 590, 630, 645, 660, 700, 780, 850, 870, 890, 910, 940, and 970 nm	GA	SVM	None	None	GA-BPNN model Identification accuracy of 100 %	Liu et al., 2022
				BPNN			GA-SVM model R_P = 0.9292 RMSEP = 0.6725 CFU/g	
Wheat kernel	DON Fusarium	1000–1650 nm	SNV (prediction)	PLSR	Regression coefficients	1198, 1322, 1353, 1428, 1445, 1497, and 1549 nm	DON R_{CV}^2 = 0.88 RMSECV = 4.8 mg/kg RPD = 4.4	Femenias et al., 2021a
			LDA Naïve Bayes K-nearest Neighbours				Classification accuracy of 100 %, 98.9 %, 98.4 %	

(*continued on next page*)

Table 2 (*continued*)

Sample	Target index	Wavelength range	Best spectral preprocessing method	Modeling algorithm	Selection method	Feature wavelengths (regions)	Best performance	Reference
Wheat kernel	DON Fusarium	900–1700 nm	1st derivative	PLSR (prediction) LDA (classification)	None	None	Intact grain $R_P^2 = 0.61$ RMSEP = 501 μg/kg Milled grain $R_P^2 = 0.59$ RMSEP = 518 μg/kg Accuracy of 85.4 %	Femenias et al., 2021b
Wheat kernel	Fusarium	940–1600 nm	SNV	LDA	None	1000, 1197, and 1394 nm	1111 nm: Accuracy range of 70–82 % 1197 nm and1395 nm: Accuracy range of 84–94 % 1000 nm, 1197 nm, and 1394 nm: Accuracy range of 85–96 %	Delwiche et al., 2021
Wheat kernel	DON Fusarium	960–1700 nm	None	Classifier model	None	None	Accuracy of 85 % for FDK Accuracy of 85 % for DON	Nadimi et al., 2021
Wheat kernel	DON	900–1700 nm	SNV	PLSR (prediction) LDA (classification)	None	None	$R_P^2 = 0.27$ RMSEP = 1174 μg/kg Accuracy of 62.7 %	Femenias et al., 2020
Wheat kernel	DON	405, 435, 450, 470, 505, 525, 570, 590, 630, 645, 660, 700, 780, 850, 870, 890, 910, 940, and 970 nm.	GA PCA	SVM (prediction) PCA-PLS (classification)	None	None	$R_P = 0.9988$ RMSEP = 365.3 μg/kg Accuracy of 94.29 %	Shi et al., 2020
Wheat kernel	Fusarium	400–1000 nm	None	RF	SPA	481,518,570,655,675,706, 726,744,764,829,852, and 925 nm	Accuracy of 96.44 %	Zhang et al., 2020
Wheat kernel	DON	363–1023 nm	None	PLSR (prediction) LDA (classification)	CARS	23 feature wavelengths	$R_P = 0.691$ RMSEP = 0.707 mg/kg accuracy of 96.92 %	Zhao et al., 2020
Wheat kernel	DON	400–1000 nm	MSC	SAE	GA	wheat kernels 430–600 nm regions	Wheat kernels accuracy of 100 %	Liang et al., 2020
Wheat flour		1000–2000 nm	SNV			wheat flour 1300–1400 nm 1500–1600 nm 1800–1950 nm	Wheat flour accuracy of 96 %	
Wheat kernel	Fusarium (F. graminearum,	400–1000 nm	None	None	None	None	Different correlation for different ranges	Alisaac et al., 2019
Wheat flour	F. culmorum, and F. poae)	1000–2500 nm						
Wheat kernel	Fusarium	938–1654 nm	None	LDA	None	1100, 1197, 1308, and 1394 nm	Classification accuracy of 96.4 %	Delwiche et al., 2019

(*continued on next page*)

Table 2 (*continued*)

Sample	Target index	Wavelength range	Best spectral preprocessing method	Modeling algorithm	Selection method	Feature wavelengths (regions)	Best performance	Reference
Wheat kernel	DON	400–1000 nm	MSC	SVM	SPA	407, 435, 636, 826, 836, 837, 847, 866, 915, 959, 973, and 999 nm	classification accuracy of 97.92 %	Liang et al., 2018
Wheat kernel	Fusarium	400–1000 nm	None	550 nm: rules. PART 710 nm: trees. LMT 850 nm: functions. LDA	None	550, 710, and 850 nm	550 nm: Classification accuracy of 94 % for variety 1 and 98 % for variety 2 710 nm: Classification accuracy of 91 % for variety 1 and 97 % for variety 2 850 nm: Classification accuracy of 85 % for variety 1 and 87 % for variety 2	Ropelewska & Zapotoczny, 2018

color, nature, and plant season (Posner, 2000). Kernel morphology is one of the most stable traits in the life history of wheat and the primary basis for identifying varieties through kernel size, shape, surface characteristics and color, which is only applied to the identification of wheat kernels with apparent differences between varieties (Mabille & Abecassis, 2003). The classification of wheat varieties is of great significance as wheat kernels with high purity guarantee wheat yield and quality. It is practical and beneficial to identify and judge different types of wheat varieties with different winter and spring characteristics, texture and color (Dubey et al., 2006). In recent years, with the decrease of hardware cost and the improvement of computing speed, imaging technology such as HIT has been widely used in the quality inspection and grading of agricultural products (Wang et al., 2023) and has been successfully applied in the variety classification of various grain crops (Feng et al., 2019).

Extensive research on HIT for identifying wheat varieties and categories has been carried out with different accuracies. Vermeulen et al. (2018) evaluated the effect of HIT as a tool for discriminating durum and common wheat kernels at single and bulk levels. The results indicated that using a combination of morphological and HIT (1100–2400 nm) and PLS-DA model led to a classification accuracy of 99 % in distinguishing between the two Italian wheat species. Although a slight spectral difference was found between conventional and waxy wheat in the 940–1650 nm range, HIT still may be used to determine the mixture levels (0–100 %) with standard errors of 9–13 percentage units, offering a potential advantage of HIT to sort wheat (Delwiche et al., 2018). The NIR spectra (900–1700 nm) preprocessed by Savitzky-Golay second derivative (SG2) were investigated by HIT combined with ANN algorithm to classify 15 Indian wheat varieties, giving a best classification accuracy of 97.77 % (Sharma et al., 2022), which is better than 93 % obtained by Tyagi et al. (2022) who identified other 16 Indian wheat varieties by HIT with the same spectral range. The same range of raw spectra without preprocessing generated a slightly better classification performance (accuracy was 99.94 %) in classifying 40 different Turkish wheat cultivars (Işık et al., 2022).

Five Chinese wheat varieties were classified by HIT combined with a nonlinear ELM algorithm, giving good classification accuracy for either full spectra (874–1734 nm) (91.3 %) or 50 feature wavelengths (87.74 %) (Bao et al., 2019). A higher classification accuracy was obtained by applying HIT to classify other 30 Chinese wheat varieties (93.01 % for full 975–1645 nm spectra, 90.20 % for 60 spectral channels) (Zhou et al., 2020). Different from the NIR range, the spectra in visible/NIR range from 400 nm to 1000 nm were studied by more researchers. Liu et al. (2020) proposed a new strategy to select 25 spectral standard deviation feature wavelength variables from the 415–995 nm range through contribution weights and categorize six close relative hybrid wheat varieties with a classification accuracy of 83.3 %. Higher accuracy was obtained from other seven research groups, who applied HIT to classify the different quantities and varieties of Chinese hybrid wheat kernels, using full 400–1000 nm range spectra or feature wavelengths, resulting in the classification accuracies ranging from 92.29 % to 99 % (details shown in Table 3), proving the great feasibility of HIT combined with chemometrics for the accurate classification and identification of wheat varieties (Zhang et al., 2022; Zhao et al., 2022; Jin et al., 2022; Que et al., 2023; Jiang et al., 2023; Zhao et al., 2023; Lei et al., 2022). In addition, Wu et al. (2021) investigated the possibility of HIT to differentiate waxy wheat and three partial waxy wheats from wild-type wheat (five wheat lines), revealing a better overall classification accuracy of 98.51 % by a SVM model based on raw spectra of 930–2548 nm, better than that by other two models.

In short, HIT can classify wheat varieties from different regions and years of different countries. HIT for wheat variety classification offers benefits such as non-destructive analysis, rapid data acquisition, and the ability to differentiate varieties based on their unique spectral fingerprints. This technology can play a crucial role in ensuring the authenticity and traceability of wheat products in the agricultural and food

Table 3
Applications of HIT for classification and identification of wheat varieties.

Sample	Target index	Wavelength range	Best spectral preprocessing method	Modeling algorithm	Selection method	Feature wavelengths (regions)	Best performance	Reference
Grain kernel	Classification of 5 Chinese grain crops (red glutinous sorghum rice, long-grain sorghum rice, long-round glutinous rice, Xikemai No. 3 wheat, home-grown corn)	397–1004.5 nm	MSC	BPNN	IVSO-CARS	41 feature wavelengths	Classification accuracies of above 99 %	Lei et al., 2022
Wheat kernel	Classification of 15 Chinese wheat varieties (vitreous wheat varieties including Jingdong8, Xinong558, Yannong19, Kenya, Wangshuibai. Piebald wheat varieties including Jinmai47, Lantian36, Junmai35, Mazhamai, Anke157. Starchy wheat varieties including Taikong6, A'bo, Mianyang26, Neixiang237, Wansu0217.)	400–1000 nm	PCA	Ensemble learning	None	None	Classification accuracy of 92.1 %	Zhao et al., 2023
Wheat kernel	Classification of 16 Indian wheat varieties (DBW 222, DBW 187, HD 3086, PBW 291, PBW 343, PBW 343 Unnat, PBW 373, PBW 658, PBW 677, PBW 725, PBW 752, PBW 771, PBW 824, PBW_550_UNNAT, PBW_Zn, PBW 766)	900–1700 nm	None	SVM	None	None	Classification accuracy of 93 %	Tyagi et al., 2023
Wheat kernel	Classification of 10 Chinese wheat varieties and mixing ratio (Mianmai 827, Mianmai 903, Mianmai 161, Mianmai 51, Chuanmai 1247, Chuannong 30, Nanmai 660, Shumai 830, Chuanmai 93, Mianmai 905)	400–1000 nm	SG-MSC	BP-Adaboost	CARS	99–145 wavelengths	Average classification accuracy of 92.29 %	Jiang et al., 2023
Wheat kernel	Classification of 8 Chinese wheat varieties (bainong4199, jimai44, zhoumai33, weilong169, Shiluan02-1, bainongAK58, xinmai26, jimai22)	400–1000 nm	None	CNN	iCR-GC	Spectral wavelength interval with 50 variables	Classification accuracy of more than 92.29 %	Que et al., 2023
Wheat seed	Classification of 20 Chinese wheat varieties from different series (Zhoumai Series, Zhengmai Series, Bainong Series, Other Series)	400–1000 nm	MSC	SVM	PCA	None	Classification accuracy of 97.64 %	Jin et al., 2022
Wheat seed	Classification of 8 Chinese wheat varieties (Bainong 4199, Bainongaikang 58, Weilong 169, Xinmai 26, Zhou Mai 33, Jimai 22, Jimai 44, Shi Luan 02–1)	400–1000 nm	None	Hybrid CNN	None	None	Classification accuracy of 95.65 %	Zhao et al., 2022
Wheat seed	Classification of 8 Chinese wheat cultivars (Jingmai 9, BS 1086, CP 730, Jingmai 11, 05Y hua 68–2, Jingmai 183, BS 237, 05Y hua 68–1)	400–1000 nm	Detrend	PLS-DA	CARS	Wavelength number < 30	Classification accuracy of more than 95 %	Zhang et al., 2022
Wheat cultivar	Classification of 40 Turkish wheat cultivars	900–1700 nm	None	CNN	None	None	Classification accuracy of 99.94 %	Işık et al., 2022
Wheat seed	Classification of 15 Indian wheat varieties (DBW187, DBW222, PBW291, PBW343, PBW343U (or PBW343 Unnat), PBW373, PBW658, PBW677, PBW725, PBW752, PBW766 (SUNHERI), PBW771, PBW824, PBW1Zn, and WH1105)	900–1700 nm	SG2	ANN	None	None	Classification accuracy of 97.77 %	Sharma et al., 2022
Waxy wheat	Discrimination of American waxy wheat (a wild-type wheat line PI 9090–1, a waxy type wheat line PI 675518, three partial waxy type wheat lines PI 9033–2, PI 9048–1, PI 9028–2)	930–2548 nm	Raw	SVM PLS-DA BPNN	None	None	Overall classification accuracy of 98.51 %, 75.76 % and 82.10 %, for the three models, respectively	Wu et al., 2021
Wheat kernel	Identification of 30 Chinese wheat varieties (aikang58, bainong207, bainong4199, bainong889, baomai218, baomai330, baomai5, fengdecunmai12, fengdecunmai20, guanmai1, huaimai20, huaimai40, huaimai41, huaimai920, jiangmai816, jiangmai919, jimai211, jimai22, lunxuan99, luomai9, ruihuamai518, saidemai1, tiechuaifu99, weilong169, xinong20, xinong979, xumai36, xumai818, yannong19, yunong035)	975–1645 nm	Normalization	CNN-ATT	CNN-FS	60 spectral channels	Classification accuracy of 93.01 % for full spectra Classification accuracy of 90.20 % for 60 spectral channels	Zhou et al., 2020
Wheat seed	Classification of six Chinese hybrid wheat varieties (Dongnongdongmai1, Dongnongdongmai2, Kechun4, Kehan16, Kenjiu10, Longfumai21)	415–995 nm	SG smoothing	SVM	SPA	25 spectral standard deviation feature variables	Classification accuracy of 83.3 %	Liu et al., 2020

(*continued on next page*)

Table 3 (*continued*)

Sample	Target index	Wavelength range	Best spectral preprocessing method	Modeling algorithm	Selection method	Feature wavelengths (regions)	Best performance	Reference
Wheat kernel	Classification of five Chinese wheat varieties (Annong1124, Longpingmai6, Shannong102, Weilong169, Zhenmai9)	874–1734 nm	Raw	ELM	RF	50 feature wavelengths	Classification accuracy of 91.3 % for full spectra and 87.74 % for feature wavelengths	Bao et al., 2019
Wheat kernel	Varieties discrimination between conventional and waxy wheat from USA	940–1650 nm	Smoothing 1st derivative 2nd derivative	PLS-DA PLS1 Pattern recognition	Regression coefficients	PLS-DA 1365, 1404,1534, and 1615 nm PLS1 1024, 1081, 1159, 1346, 1418, 1500, and 1610 nm	Standard errors of 9–13 percentage units	Delwiche et al., 2018
Wheat kernel	Species discrimination between durum and common wheat from Italy	1100–2400 nm	None	PLS-DA	None	None	Classification accuracy of 99 %	Vermeulen et al., 2018

industries. Based on the current research results, continuous improvements in HIT for classifying and identifying wheat varieties are essential to enhance accuracy, reliability, and practicality.

3.4. Identification of non-mildew damage in wheat kernels

In addition to the damage caused by mildew, wheat kernels suffer damage from other factors such as sprouting, black points, broken wrinkles and parasites. Sprouting in wheat kernels often occurs after rain and is usually caused by mismanagement after harvest, including delayed drying, improper storage, and harvesting too late, and so on, which easily results in unpleasant effects of rancidity, nutrient loss, taste change of wheat kernels, reducing wheat quality and commodity value (Gabrovská et al., 2007). Sprouted kernels are vulnerable to infestations by diseases and insects (Singh et al., 2009) and should be inspected in a timely manner to minimize the loss caused by the infected damages. HIT can provide spectra for each pixel in an image. It was explored for its potential to detect sprout damage in wheat kernels using a 528–1785 nm wavelength range for discriminating between sound and sprouted kernels. A global threshold value of 0.30 was used to separate sound and sprouted kernels, achieving an accuracy of 100 % for the three wheat cultivars tested (Barbedo et al., 2018). Hyperspectral images of both sides of wheat kernels were also acquired to identify sound and slightly sprouted wheat kernels. Classification modeling was performed using a machine learning deep forest (DF) algorithm, indicating slightly better effects of spectral data from the reverse side compared to those from the ventral side. By applying the full 254 wavelengths and the 29 characteristic wavelengths selected from the reverse side by CARS algorithm, a good classification accuracy of 94.5 % and 93 % was generated, respectively, to exhibit the practicality and usefulness of HIT in identifying sprouted wheat kernels (Zhang et al., 2020). The hyperspectral images of healthy wheat grain, germinated wheat grain, and shriveled wheat grain with two sides were investigated and the classification accuracy was tested using a SVM model. The results showed a classification accuracy of 98.5 % for the reverse side (with 7 characteristic wavelengths) and 97.4 % for the ventral side (with 6 characteristic wavelengths) (Zhang & Ji, 2019), slightly better than that by the CNN model, based on the identical spectra (866.4–1701 nm) (Li et al., 2022), indicating a good prospect of HIT in the identification of unsound wheat kernels.

Wheat kernels damaged with the occurrence of black points, broken, and wrinkles were also discriminated from healthy wheat kernels by HIT. With full spectra (900–1700 nm, 160 wavelengths) and 8 effective wavelengths selected by X-loadings and SPA methods, three non-linear LS-SVM models were developed to classify damaged wheat kernels and achieved a perfect classification accuracy of 100 %, better than linear PLS models (97.2 %–98.9 %) (Shao et al., 2020). More wheat kernel samples with different degrees of damage are still required to increase the robust discrimination.

Rice-weevil, one of the most common pests, is mainly parasitized in stored grains, such as rice, corn, wheat, barley, and sorghum (Tripathi, 2018). Rice-weevil is very harmful and easily causes quality degradation of wheat kernels (Singh & Sharma, 2021). Manual screening is always used to visually detect and identify pest-damaged wheat kernels, which is inefficient, subjective, low-precision, and very difficult to use to detect high-quality wheat kernels in large quantities. For this reason, developing a rapid method to achieve the detection more objectively and accurately is necessary. Zhang et al., (2021) proposed to use HIT in tandem with LDA to identify rice-weevil-damaged wheat kernels from the four sides (reverse, ventral, and two flanks). Using eight feature wavelengths selected from the 866.4–1701 nm range, a LDA model was established and validated with high accuracy, sensitivity and specificity (97 %, 98 %, and 96 %, respectively), indicating the reliability of HIT to identify the sound and Rice-weevil-damaged wheat kernels. All the specific research results are shown in Table 4.

To sum up, detecting non-mildew damage in wheat kernels by HIT is

Table 4
Applications of HIT for identification of non-mildew damage in wheat kernels.

Sample	Target index	Wavelength range	Best spectral preprocessing method	Modeling algorithm	Selection method	Feature wavelengths (regions)	Best performance	Reference
Wheat kernel	Germinated wheat grain Shriveled wheat grain	866.4–1701 nm	None	CNN	None	None	Accuracy increased from 79.17 % to 96.67 %	Li et al., 2022
Wheat kernel	Rice-weevil	866.4–1701 nm	SNV	LDA	SPA	8 wavelengths	Accuracy, sensitivity and specificity of 97 %, 98 % and 96 %, respectively.	Zhang et al., 2021
Wheat kernel	Slightly sprout	866.4–1701 nm	S-G smoothing	DF	CARS	976.4, 986.6, 1024.1, 1027.5, 1030.9, 1044.5, 1047.9, 1088.5, 1091.8, 1098.6, 1102, 1118.8, 1122.2, 1125.5, 1128.9, 1132.3, 1155.7, 1159.1, 1169.1, 1209.2, 1245.8, 1288.8, 1361.1, 1364.4, 1423.1, 1445.8, 1526.4, 1529.6, and 1564.8 nm	Full wavelengths (254) Classification accuracy of 94.5 % Feature wavelengths (29) Classification accuracy of 93 %	Zhang et al., 2020
Wheat kernel	Black point Broken	900–1700 nm	PCA	LS-SVM	X-loadings	X-loadings 937, 965, 1129, 1176, 1217, 1340, 1411, and 1677 nm	LS-SVM Classification accuracy of 100 %	Shao et al., 2020
	Wrinkle Healthy			PLS	SPA	SPA 935, 961, 1130, 1207, 1300, 1370, 1449, and 1672 nm	PLS Classification accuracy of 100 %	
Wheat kernel	Germinated wheat grain Shriveled wheat grain	866.4–1701 nm	MSC	SVM	PC loading	Reverse side 1105.3, 1199.2, 1305.3, 1321.7, 1439.3, 1458.7, and 1478.1 nm Ventral side 1112.1, 1202.5, 1298.7, 1341.4, 1458.7, and 1484.6 nm	Reverse side Average classification accuracy of 98.5 % Ventral side Average classification accuracy of 97.4 %	Zhang & Ji, 2019
Wheat kernel	Sprout	528–1785 nm	None	None	None	None	Classification accuracy of 97.2–98.9 %	Barbedo et al., 2018

possible and would benefit wheat kernels' grade and post-harvest processing. HIT and advanced data analysis techniques can provide a reliable and non-destructive method for identifying non-mildew damage in wheat kernels. The ability to detect subtle variations in spectral signatures enables precise discrimination between healthy and damaged kernels, contributing to quality control in the wheat industry. Dealing with the process of HIT discrimination, it is important to continually address challenges such as data analysis complexity, calibration requirements, and ensuring the robustness of the technology in diverse environmental conditions. As technology continues to evolve, the trend of employing portable miniature instruments in food and agriculture will likely grow, offering new possibilities for improved crop management and quality control (Zhu et al., 2022). Portable miniature HIT sensors for detecting damaged wheat kernels should be considered and developed in the future.

3.5. Detection of wheat flour adulteration

Wheat flour is a powder made from wheat kernels, rich in carbohydrates, protein and various vitamins, and provides energy and nutrients for the human body (Atwell & Finnie, 2016). Wheat flour has been an indispensable ingredient in our daily life. It has often been used as one of the main raw materials to make pasta, pastry and other foods since ancient times, playing a role in alleviating hunger, increasing satiety and taste, supplementing nutrition, and promoting digestion and absorption (Shewry & Hey, 2015).

In order to improve the appearance of wheat flour and reduce costs, there are still some inappropriate or illegal behaviors in the market, such as the use of low-cost, substandard raw materials or the addition of inferior raw materials in flour to increase profits, which often results in poor nutrition, taste and safety issues of flour. According to the reports, flour adulterants often include talcum powder, benzoyl peroxide (BPO), and other powders (Pastor, Ačanski, & Vujić, 2019). Using HIT to identify and detect these adulterants is of great practical significance. Zhao et al. (2019) investigated the potential of HIT combined with a small number of feature wavelengths (<10, 1158–1700 nm) to detect low-level peanut powder (0.01–10 %, w/w) mixed in different varieties of whole wheat flour. For both spring and winter wheat flour, the peanut powder in the low concentration was detected with high precision ($R_P^2 >$ 0.99). Defatted peanut flour with a concentration range from 0.02 % to 20 % mixed in wheat flour was used to verify the detection performance of HIT in tandem with a developed Matched Subspace Detector (MSD) algorithm and a global adulteration of 0.2 % of peanut in wheat flour proved the best detection accuracy (Laborde et al., 2020). HIT was used to detect two adulterants, peanut flour and walnut flour, mixed in wheat flour and achieved excellent performance ($R_P^2 = 0.987$, RMSEP = 0.373 %) along with a detection limit as low as 1 % (Zhao et al., 2018). In another study, three adulterants, such as BPO + alloxan monohydrate + L-cysteine (0.05–1.5 %, w/w) mixed in wheat flour was also detected with a high precision (R > 0.98), using Raman HIT in short wave NIR region (740–1010 nm) (Lohumi et al., 2019). Similarly, a high accuracy of over 92.45 % was observed in detecting another combination of three adulterants (BPO + peanut flour + walnut flour) in wheat flour (Zheng et al., 2022).

Several countries, especially the European Union and China, have banned talcum powder and BPO in wheat flour production (Liu et al., 2023). Talcum powder is white and tasteless and can be used to improve the flour appearance. The appropriate addition of BPO as a bleaching agent can enhance the flour's appearance and storage. Using HIT combined only four feature wavelengths (907.135, 1339.866, 1392.573, 1394.22 nm) to detect wheat flour adulterated with talcum powder has yielded good results ($R_P = 0.98$, RMSEP = 2.88 %) (He et al., 2023).

With eight feature wavelength regions involved, a short-wave HIT system was developed to detect BPO content (50–6400 ppm) in wheat flour with high accuracy ($R_P^2 > 0.985$) (Kim et al., 2022). In addition to being successfully detected individually, these two indicators can be predicted when combined. Talcum powder mixed with BPO, as binary adulterants at low levels (<5.0 %) in wheat flour was effectively discriminated by HIT in the 900–1700 nm range combined with different spectral analysis methods (Fu et al., 2020; Fu et al., 2021) (shown in Table 5). In general, adulterants at low levels can be detected by HIT with good accuracy, which demonstrates a high potential of HIT for discriminating different powder particles in wheat flour.

It is worth noting that HIT provides a detailed spectral signature for each pixel in an image, covering a broad NIR range of wavelengths, for wheat flour quality analysis, with different performance achieved for different range data, which is mainly due to the interaction between NIR spectra and different functional groups of biomacromolecules of wheat compositions. After being absorbed by the NIR light, the spectral points located at different locations produce different vibrations and overtones for these chemical groups (Zhang et al., 2022). The main components of wheat flour include water, starch, protein, ash, and some functional substances, which are closely related to its nutritional and processing properties. The hydrogen-containing groups such as O—H, N—H, C—H, S—H bonds in wheat flour components have characteristic absorption peaks in NIR region, which is the basis of HIT to detect the chemical composition of wheat flour (Salgó & Gergely, 2012). The absorption bands in NIR region are sensitive to the chemical compositions of wheat flour, and the presence of adulterants may introduce spectral interference, causing overlapping or shifting of absorption bands in the NIR spectra, which complicate the interpretation of the spectra and require advanced data analysis techniques, commonly including chemometrics and machine learning algorithms, to extract relevant information from the spectra, and distinguish and quantify different adulterants in wheat flour (Liu et al., 2023). The impact of adulterants on NIR spectra depends on various factors, such as the type and concentration of adulterants, the specific characteristics of wheat flour, and the measurement conditions. Detection and analysis of adulterants in wheat flour using HIT often involve comparing observed spectra with reference spectra of known adulterants or using chemometric models trained on authentic

Table 5
Applications of HIT for detection of wheat flour adulteration.

Sample	Target index	Wavelength range	Best spectral preprocessing method	Modeling algorithm	Selection method	Feature wavelengths (regions)	Best performance	Reference
Wheat flour	Talcum powder	900–1700 nm	SNV	PLSR	CARS	907.135, 1339.866, 1392.573, and 1394.22 nm	$R_P = 0.98$ RMSEP = 2.88 % RPD = 5.09	He et al., 2023
Wheat flour	BPO	1000–2500 nm	Smoothing, mean normalization, maximum normalization, range normalization, MSC, SNV, Savitzky–Golay 1st derivative, Savitzky–Golay 2nd derivative	PLSR	RMSEV values	937.5–1062.5 nm, 1062.5–1187.5 nm, 1312.5–1436.5 nm, 1436.5–1562.5 nm, 1562.5–1687.5 nm, 1812.5–1937.5 nm, 1937.5–2062.5 nm, 2062.5–2187 nm	$R_P^2 > 0.985$	Kim et al., 2022
Wheat flour	Peanut flour Walnut flour BPO	380–1030 nm	None	gcForest	EMCVS	487, 704, and 883 nm	Accuracy > 92.45 %	Zheng et al., 2022
Wheat flour	Talcum powder BPO	900–1700 nm	mean-centre normalisation, 1st derivative	None	None	None	None	Fu et al., 2021
Wheat flour	Defatted peanut flour	1200–2200 nm	S-G smoothing, SNV	MSD algorithm	None	None	Detection concentration of 0.2 %	Laborde et al., 2020
Wheat flour	Talcum powder BPO	900–1700 nm	mean-centred normalisation, 1st derivative	Talcum powder 1st derivative band difference method BPO spectral correlation measurement	None	None	Detection concentration of 0.02–5 %	Fu et al., 2020
Wheat flour	peanut powder	1158–1700 nm	S-G + 1st derivatives SNV	PLSR	CARS	Spring wheat flour 1,196, 1,354, 1,411, 1,478, 1,482, 1,492, and 1545 nm Winter wheat flour 1,200, 1,203, 1,242, 1,245, and 1249 nm	Spring wheat flour $R_P^2 = 0.993$ RMSEP = 0.251 % Winter wheat flour $R_P^2 = 0.991$ RMSEP = 0.285 %	Zhao et al., 2019
Wheat flour	BPO Alloxan monohydrate L-cysteine	740–1010 nm	None	SAM	None	None	R > 0.98 Detection concentration of 0.05–1.5 % (w/w)	Lohumi et al., 2019
Wheat flour	Peanut powder Walnut powder	950–1700 nm	SNV + 1st Der	PLSR	SPA, UVE	SPA 1064, 1127, 1203, 1365, 1368, 1464, 1574, 1581, 1585, 1606, 1624 UVE 1022, 1186, 1193, 1196, 1200, 1203, 1207, 1210, 1231, 1249, 1252, 1256 1372, 1390, 1606, 1613, 1638	SPA $R_P^2 = 0.960$ RMSEP = 0.645 % UVE $R_P^2 = 0.987$ RMSEP = 0.373 %	Zhao et al., 2018

samples. The imaging function in HIT allows for the spatial visualization of adulterant changes in terms of concentration and distribution in wheat flour.

Compared with other imaging techniques, such as computer vision (Goyal, Kumar, & Verma, 2022), HIT offers unique advantages for detecting flour adulteration, such as detailed spectral information and spatial resolution. X-ray and CT imaging may offer better penetration depth and can be more effective in detecting internal structures and foreign objects (Sivakumar et al., 2023), but is rarely used. Although, HIT still comes with challenges related to data complexity, equipment cost, and specific calibration requirements. Continuous research and development efforts, along with advancements in technology and methodology, are essential for improving the capabilities of HIT in detecting flour adulteration. The software and hardware improvements will contribute to the overall reliability, accuracy, and applicability of hyperspectral imaging systems in the food industry.

4. Limitations and challenges

Although HIT has been studied and proven to possess great potential for the quality evaluation of wheat quality, a lot of research is still required before achieving the real industrial detection application of wheat quality. Some restrictions and challenges remain and should be addressed to overcome the existing barriers (shown in Fig. 4). Firstly, HIT has achieved certain valuable results in detecting the main chemical components such as ash, protein, starch, moisture and other micronutrients of wheat grains, but few or no outcomes of stability time, cellulose, thousand-grain weight, and precipitation value. Besides, HIT also has some problems in the classification and identification of wheat varieties in terms of effectiveness and stability, originating from the inconsistencies of samples, which is mainly caused by planting region, production year, storage conditions, transportation and circulation environments, increasing the difficulty and uncertainty of HIT modeling. As the characteristic wavelengths vary for different wheat varieties, there is still a problem of low reliability of established models in the qualitative identification or quantitative determination of wheat quality by HIT.

Secondly, there are limitations in the functionality of HIT equipment used for assessing wheat quality. Current devices cannot simultaneously acquire spectra, process data, and perform intelligent analysis. Additionally, HIT equipment suitable for laboratory use is bulky and challenging to transport for field use. The processing speed for vast amounts of HIT data varies significantly with software versions, resulting in the non-universality of a constructed model. This variability hampers the universal application of HIT in wheat quality assessment.

Finally, the existing HIT equipment is still expensive, compared with other detection techniques, because of the high cost of sophisticated spectrometers and high-definition cameras embedded in the HIT system. Due to the huge amount of data collected by HIT systems, more storage and processing power, that is, computing power, is required. This requirement directly impacts the broader adaptation and future application of HIT. It is worth noting that the resolution of hyperspectral images collected from the HIT system is limited because HIT requires more spectral bands and the image resolution of each band is relatively low, which may influence the data accuracy and application of HIT. HIT demands specific working conditions, particularly about lighting. Adequate illumination is essential for effective HIT operation; without it, imaging quality may be compromised, requiring additional effort in data processing. This requirement for optimal lighting conditions is a significant factor in the practical use of HIT.

5. Trends and future prospects

Scientists are expecting many significant advancements in HIT in the coming days. One of the key developments in this technology would be the miniaturization of hyperspectral cameras and sensors. Current HIT devices are bulky and expensive. Miniaturization would make this technology more accessible and affordable for a wide range of applications for the end users (Kamruzzaman, 2023). Smaller and cheaper cameras may be integrated into many consumer devices like smartphones. Electronic and sensor devices are rapidly growing, and these advancements are expected to lead to the development of more advanced hyperspectral cameras with higher spectral and spatial resolution. This will allow for capturing more detailed and precise image data from the tested objects. Ultimately, it will help to improve the sensitivity to detect subtle differences in the spectral signatures for various applications. ML/AI fields are rapidly evolving, and integrating ML/AI with HIT data will likely become more common in the coming days. Due to miniaturization and lightweight hyperspectral cameras, more field applications are expected. Drones equipped with hyperspectral cameras can cover large areas very quickly. The manufacturers will use miniature hyperspectral cameras in various processing and

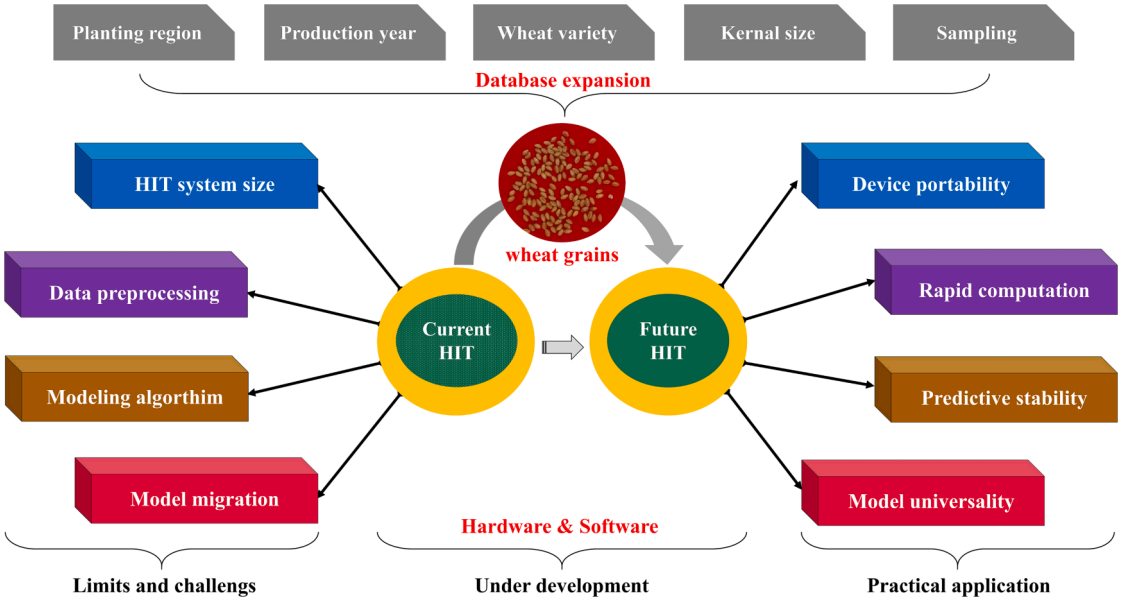

Fig. 4. Limitations, challenges, developing trends, and future prospects of HIT in the evaluation of wheat quality.

production systems stages for real-time data processing capabilities, better visualization, and user-friendly interfaces for various applications. These anticipated developments reflect a trend towards more versatile, efficient, and accessible HIT, with potential impacts across various fields and industries.

CRediT authorship contribution statement

Yuling Wang: Methodology, Formal analysis, Investigation, Writing - original draft, Writing - review & editing. **Xingqi Ou:** Resources, Project administration, Funding acquisition. Writing - review & editing. **Hong-Ju He:** Conceptualization, Writing - review & editing, Supervision, Funding acquisition. **Mohammed Kamruzzaman:** Writing – review & editing, Writing – original draft, Conceptualization.

Declaration of competing interest

The authors declare that they have no known competing financial interests or personal relationships that could have appeared to influence the work reported in this paper.

Data availability

No data was used for the research described in the article.

Acknowledgments

The authors acknowledge that this work was financially supported by Henan Province Key Science and Technology Project (No. 221100110300), and Henan Institute of Science and Technology Cooperation Project (No. 2021410707000060).

References

Abdel-Aal, E. S., Sosulski, F. W., & Hucl, P. (1998). Origins, characteristics, and potentials of ancient wheats. *Cereal Foods World, 43*(9), 708–715.
Abedi, E., & Pourmohammadi, K. (2021). Physical modifications of wheat gluten protein: An extensive review. *Journal of Food Process Engineering, 44*(3), e13619.
Acevedo, E., Silva, P., & Silva, H. (2002). Bread wheat: Improvement and production, wheat growth and physiology. *FAO plant production and protection series*. Food and Agriculture Organization of the United Nations.
Ahmed, E., Sulaiman, J., & Mohd, S. (2011). Wheat production and economics. *American Journal of Agricultural and Biological Sciences, 6*(3), 332–338.
Alisaac, E., Behmann, J., Rathgeb, A., Karlovsky, P., Dehne, H. W., & Mahlein, A. K. (2019). Assessment of Fusarium infection and mycotoxin contamination of wheat kernels and flour using hyperspectral imaging. *Toxins, 11*(10), 556.
An, D., Zhang, L., Liu, Z., Liu, J., & Wei, Y. (2023). Advances in infrared spectroscopy and hyperspectral imaging combined with artificial intelligence for the detection of cereals quality. *Critical Reviews in Food Science and Nutrition, 63*(29), 9766–9796.
Atwell, W. A., & Finnie, S. (2016). *Wheat flour*. Elsevier.
Banach, J. K., Majewska, K., & Żuk-Gołaszewska, K. (2021). Effect of cultivation system on quality changes in durum wheat grain and flour produced in North-Eastern Europe. *Plos one, 16*(1), Article e0236617.
Bao, Y., Mi, C., Wu, N., Liu, F., & He, Y. (2019). Rapid classification of wheat grain varieties using hyperspectral imaging and chemometrics. *Applied Sciences, 9*(19), Article 4119.
Barbedo, J. G., Guarienti, E. M., & Tibola, C. S. (2018). Detection of sprout damage in wheat kernels using NIR hyperspectral imaging. *Biosystems Engineering, 175*, 124–132.
Beccari, G., Caproni, L., Tini, F., Uhlig, S., & Covarelli, L. (2016). Presence of Fusarium species and other toxigenic fungi in malting barley and multi-mycotoxin analysis by liquid chromatography–high-resolution mass spectrometry. *Journal of Agricultural and Food Chemistry, 64*(21), 4390–4399.
Campillo, R., Jobet, C., & Undurraga, P. (2010). Effects of nitrogen on productivity, grain quality, and optimal nitrogen rates in winter wheat cv. Kumpa-INIA in Andisols of Southern Chile. *Chilean Journal of Agricultural Research, 70*(1), 122–131.
Caporaso, N., Whitworth, M. B., & Fisk, I. D. (2018). Protein content prediction in single wheat kernels using hyperspectral imaging. *Food Chemistry, 240*, 32–42.
Cimbalo, A., Alonso-Garrido, M., Font, G., & Manyes, L. (2020). Toxicity of mycotoxins in vivo on vertebrate organisms: A review. *Food and Chemical Toxicology, 137*, Article 111161.
Cornell, H., & Hoveling, A. W. (2020). *Wheat: Chemistry and utilization*. CRC Press.
da Rocha, M. E. B., Freire, F. D. C. O., Maia, F. E. F., Guedes, M. I. F., & Rondina, D. (2014). Mycotoxins and their effects on human and animal health. *Food Control, 36*(1), 159–165.
Davies, E. R. (2017). *Computer vision: Principles, algorithms, applications, learning*. Academic Press.
Delwiche, S. R., Baek, I., & Kim, M. S. (2021). Does spatial region of interest (ROI) matter in multispectral and hyperspectral imaging of segmented wheat kernels? *Biosystems Engineering, 212*, 106–114.
Delwiche, S. R., Qin, J., Graybosch, R. A., Rausch, S. R., & Kim, M. S. (2018). Near infrared hyperspectral imaging of blends of conventional and waxy hard wheats. *Journal of Spectral Imaging, 7*.
Delwiche, S. R., Rodriguez, I. T., Rausch, S. R., & Graybosch, R. A. (2019). Estimating percentages of fusarium-damaged kernels in hard wheat by near-infrared hyperspectral imaging. *Journal of Cereal Science, 87*, 18–24.
De Santis, M. A., Soccio, M., Laus, M. N., & Flagella, Z. (2021). Influence of drought and salt stress on durum wheat grain quality and composition: A review. *Plants, 10*(12), 2599.
Dexter, J. E., Williams, P. C., Edwards, N. M., & Martin, D. G. (1988). The relationships between durum wheat vitreousness, kernel hardness and processing quality. *Journal of Cereal Science, 7*, 169–181.
Dhakal, K., Sivaramakrishnan, U., Zhang, X., Belay, K., Oakes, J., Wei, X., & Li, S. (2023). Machine learning analysis of hyperspectral images of damaged wheat kernels. *Sensors, 23*(7), 3523.
Dinu, M., Whittaker, A., Pagliai, G., Benedettelli, S., & Sofi, F. (2018). Ancient wheat species and human health: Biochemical and clinical implications. *The Journal of Nutritional Biochemistry, 52*, 1–9.
Du, Z., Tian, W., Tilley, M., Wang, D., Zhang, G., & Li, Y. (2022). Quantitative assessment of wheat quality using near-infrared spectroscopy: A comprehensive review. *Comprehensive Reviews in Food Science and Food Safety, 21*(3), 2956–3009.
Dubey, B. P., Bhagwat, S. G., Shouche, S. P., & Sainis, J. K. (2006). Potential of artificial neural networks in varietal identification using morphometry of wheat grains. *Biosystems Engineering, 95*(1), 61–67.
Erkinbaev, C., Derksen, K., & Paliwal, J. (2019). Single kernel wheat hardness estimation using near infrared hyperspectral imaging. *Infrared Physics & Technology, 98*, 250–255.
FAO/FAOSTAT, 2021. Statistics division of food and agriculture Organization of the United Nations. https://www.fao.org/faostat/en/#data/QCL/visualize.
Femenias, A., Bainotti, M. B., Gatius, F., Ramos, A. J., & Marín, S. (2021a). Standardization of near infrared hyperspectral imaging for wheat single kernel sorting according to deoxynivalenol level. *Food Research International, 139*, Article 109925.
Femenias, A., Gatius, F., Ramos, A. J., Sanchis, V., & Marín, S. (2021b). Near-infrared hyperspectral imaging for deoxynivalenol and ergosterol estimation in wheat samples. *Food Chemistry, 341*, Article 128206.
Femenias, A., Gatius, F., Ramos, A. J., Sanchis, V., & Marín, S. (2020). Standardisation of near infrared hyperspectral imaging for quantification and classification of DON contaminated wheat samples. *Food Control, 111*, Article 107074.
Femenias, A., Llorens-Serentill, E., Ramos, A. J., Sanchis, V., & Marín, S. (2022). Near-infrared hyperspectral imaging evaluation of fusarium damage and DON in single wheat kernels. *Food Control, 142*, Article 109239.
Feng, L., Zhu, S., Liu, F., He, Y., Bao, Y., & Zhang, C. (2019). Hyperspectral imaging for seed quality and safety inspection: A review. *Plant Methods, 15*(1), 1–25.
Filip, E., Woronko, K., Stępień, E., & Czarniecka, N. (2023). An overview of factors affecting the functional quality of common wheat (Triticum aestivum L.). *International Journal of Molecular Sciences, 24*(8), 7524.
Fu, X., Chen, J., Fu, F., & Wu, C. (2020). Discrimination of talcum powder and benzoyl peroxide in wheat flour by near-infrared hyperspectral imaging. *Biosystems Engineering, 190*, 120–130.
Fu, X., Chen, J., Zhang, J., Fu, F., & Wu, C. (2021). Effect of penetration depth and particle size on detection of wheat flour adulterant using hyperspectral imaging. *Biosystems Engineering, 204*, 64–78.
Gabrovská, D., Strohalm, J., Paulíčková, I., Maškova, E., Fiedlerová, V., Holasová, M., & Houška, M. (2007). Nutritional and sensory quality of selected sprouted seeds. *High Pressure Research, 27*(1), 143–146.
Geren, H. (2021). Wheat importance, history and adaptation. In M. Karaman (Ed.), *Theoretical and practical new approach in cereal science and technology* (pp. 3–24). Iksad Publishing House.
Goyal, K., Kumar, P., & Verma, K. (2022). Food adulteration detection using artificial intelligence: A systematic review. *Archives of Computational Methods in Engineering, 29*(1), 397–426.
Hazard, B., Trafford, K., Lovegrove, A., Griffiths, S., Uauy, C., & Shewry, P. (2020). Strategies to improve wheat for human health. *Nature Food, 1*(8), 475–480.
He, H. J., Chen, Y., Li, D. G., Wang, Y., Ou, X., & Guo, J. (2023). Hyperspectral imaging combined with chemometrics for rapid detection of talcum powder adulterated in wheat flour. *Food Control, 144*, Article 109378.
He, H. J., & Sun, D. W. (2015). Hyperspectral imaging technology for rapid detection of various microbial contaminants in agricultural and food products. *Trends in Food Science & Technology, 46*(1), 99–109.
Hershman, D., Shaner, G., & Van Sanford, D. (2012). A unified effort to fight an enemy of wheat and barley: Fusarium Head Blight. *Plant Disease, 96*(12), Article 17121728.
Hu, N., Li, W., Du, C., Zhang, Z., Gao, Y., Sun, Z., & Wang, Z. (2021). Predicting micronutrients of wheat using hyperspectral imaging. *Food Chemistry, 343*, Article 128473.
Igrejas, G., & Branlard, G. (2020). The importance of wheat. Wheat quality for improving processing and human health, 1-7.
Iqbal, M. J., Shams, N., & Fatima, K. (2022). Nutritional quality of wheat. *Wheat*. IntechOpen.

Iqbal, Z., Pasha, I., Abrar, M., Masih, S., & Hanif, M. S. (2015). Physico-chemical, functional and rheological properties of wheat varieties. *Journal of Agricultural Research, 53*(2), 253–267.
Işık, Ş., Özkan, K., Demirez, D. Z., & Seke, E. (2022). Consensus rule for wheat cultivar classification on VL, VNIR and SWIR imaging. *IET Image Processing, 16*(11), 2834–2844.
Jayas, D. S., Paliwal, J., Erkinbaev, C., Ghosh, P. K., & Karunakaran, C. (2016). Wheat quality evaluation. In *Computer vision technology for food quality evaluation* (pp. 385–412). Academic Press.
Jiang, X., Bu, Y., Han, L., Tian, J., Hu, X., Zhang, X., & Luo, H. (2023). Rapid nondestructive detecting of wheat varieties and mixing ratio by combining hyperspectral imaging and ensemble learning. *Food Control, 150*, Article 109740.
Jin, S., Zhang, W., Yang, P., Zheng, Y., An, J., Zhang, Z., & Pan, X. (2022). Spatial-spectral feature extraction of hyperspectral images for wheat seed identification. *Computers and Electrical Engineering, 101*, Article 108077.
Kamruzzaman, M. (2023). Optical sensing as analytical tools for meat tenderness measurements - A review. *Meat Science, 195*, 109007.
Kamruzzaman, M., Makino, Y., & Oshita, S. (2015). Non-invasive analytical technology for the detection of contamination, adulteration, and authenticity of meat, poultry, and fish: A review. *Analytica Chimica Acta, 853*, 19–29.
Kim, G., Lee, H., Baek, I., Cho, B. K., & Kim, M. S. (2022). Quantitative detection of benzoyl peroxide in wheat flour using line-scan short-wave infrared hyperspectral imaging. *Sensors and Actuators B: Chemical, 352*, Article 130997.
Knapp, S., Brabant, C., Oberforster, M., Grausgruber, H., & Hiltbrunner, J. (2017). Quality traits in winter wheat: Comparison of stability parameters and correlations between traits regarding their stability. *Journal of Cereal Science, 77*, 186–193.
Kovač, M., Bulaić, M., Jakovljević, J., Nevistić, A., Rot, T., Kovač, T., & Šarkanj, B. (2021). Mycotoxins, pesticide residues, and heavy metals analysis of Croatian cereals. *Microorganisms, 9*(2), 216.
Kucek, L. K., Dyck, E., Russell, J., Clark, L., Hamelman, J., Burns-Leader, S., & Dawson, J. C. (2017). Evaluation of wheat and emmer varieties for artisanal baking, pasta making, and sensory quality. *Journal of Cereal Science, 74*, 19–27.
Laborde, A., Jaillais, B., Roger, J. M., Metz, M., Bouveresse, D. J. R., Eveleigh, L., & Cordella, C. (2020). Subpixel detection of peanut in wheat flour using a matched subspace detector algorithm and near-infrared hyperspectral imaging. *Talanta, 216*, Article 120993.
Lasztity, R., & Abonyi, T. (2009). Prediction of wheat quality—past, present, future. *A review. Food Reviews International, 25*(2), 126–141.
Lei, Y., Hu, X., Tian, J., Zhang, J., Yan, S., Xue, Q., & Huang, D. (2022). Rapid resolution of types and proportions of broken grains using hyperspectral imaging and optimisation algorithm. *Journal of Cereal Science*, Article 103565.
Li, H., Zhang, L., Sun, H., Rao, Z., & Ji, H. (2022). Discrimination of unsound wheat kernels based on deep convolutional generative adversarial network and near-infrared hyperspectral imaging technology. *Spectrochimica Acta Part A: Molecular and Biomolecular Spectroscopy, 268*, Article 120722.
Li, J., Zhang, S., Liu, C., Yin, Y., Sun, X., & Wu, J. (2023). Characterization of ash content in wheat flour using data fusion. *Infrared Physics & Technology*, Article 104792.
Liang, K., Huang, J., He, R., Wang, Q., Chai, Y., & Shen, M. (2020). Comparison of Vis-NIR and SWIR hyperspectral imaging for the non-destructive detection of DON levels in Fusarium head blight wheat kernels and wheat flour. *Infrared Physics & Technology, 106*, Article 103281.
Liang, K., Liu, Q. X., Xu, J. H., Wang, Y. Q., Okinda, C. S., & Shena, M. X. (2018). Determination and visualization of different levels of deoxynivalenol in bulk wheat kernels by hyperspectral imaging. *Journal of Applied Spectroscopy, 85*, 953–961.
Litvinov, D. Y., Karlov, G. I., & Divashuk, M. G. (2021). Metabolomics for crop breeding: General considerations. *Genes, 12*(10), 1602.
Liu, H. Y., Wadood, S. A., Xia, Y., Liu, Y., Guo, H., Guo, B. L., & Gan, R. Y. (2023). Wheat authentication: An overview on different techniques and chemometric methods. *Critical Reviews in Food Science and Nutrition, 63*(1), 33–56.
Liu, J., Liu, S., Shi, T., Wang, X., Chen, Y., Liu, F., & Men, H. (2020). A modified feature fusion method for distinguishing seed strains using hyperspectral data. *International Journal of Food Engineering, 16*(7), Article 20190362.
Liu, W., He, L., Xia, Y., Ren, L., Liu, C., & Zheng, L. (2022). Monitoring the growth of Fusarium graminearum in wheat kernels using multispectral imaging with chemometric methods. *Analytical Methods, 14*(2), 106–113.
Lohumi, S., Lee, H., Kim, M. S., Qin, J., & Cho, B. K. (2019). Raman hyperspectral imaging and spectral similarity analysis for quantitative detection of multiple adulterants in wheat flour. *Biosystems Engineering, 181*, 103–113.
Lv, Y., Lv, W., Han, K., Tao, W., Zheng, L., Weng, S., & Huang, L. (2022). Determination of wheat kernels damaged by fusarium head blight using monochromatic images of effective wavelengths from hyperspectral imaging coupled with an architecture self-search deep network. *Food Control, 135*, Article 108819.
Mabille, F., & Abecassis, J. (2003). Parametric modelling of wheat grain morphology: A new perspective. *Journal of Cereal Science, 37*(1), 43–53.
Mitchell, D. O., & Mielke, M. (2005). Wheat: The global market, policies, and priorities. *Global Agricultural Trade and Developing Countries*, 195–214.
Mohapatra, D., Kumar, S., Kotwaliwale, N., & Singh, K. K. (2017). Critical factors responsible for fungi growth in stored food grains and non-Chemical approaches for their control. *Industrial Crops and Products, 108*, 162–182.
Morales-Sillero, A., Pierna, J. A. F., Sinnaeve, G., Dardenne, P., & Baeten, V. (2018). Quantification of protein in wheat using near infrared hyperspectral imaging: Performance comparison with conventional near infrared spectroscopy. *Journal of Near Infrared Spectroscopy, 26*(3), 186–195.
Nadimi, M., Brown, J. M., Morrison, J., & Paliwal, J. (2021). Examination of wheat kernels for the presence of Fusarium damage and mycotoxins using near-infrared hyperspectral imaging. *Measurement: Food, 4*, Article 100011.
Njira, K. O., & Nabwami, J. (2015). A review of effects of nutrient elements on crop quality. *African Journal of Food, Agriculture, Nutrition and Development, 15*(1), 9777–9793.
Oliveira, I. S., da Silva Junior, A. G., de Andrade, C. A. S., & Oliveira, M. D. L. (2019). Biosensors for early detection of fungi spoilage and toxigenic and mycotoxins in food. *Current Opinion in Food Science, 29*, 64–79.
Ooms, N., & Delcour, J. A. (2019). How to impact gluten protein network formation during wheat flour dough making. *Current Opinion in Food Science, 25*, 88–97.
Ortolan, F., & Steel, C. J. (2017). Protein characteristics that affect the quality of vital wheat gluten to be used in baking: A review. *Comprehensive Reviews in Food Science and Food Safety, 16*(3), 369–381.
Pacheco-Gil, R. A., Velasco-Cruz, C., Pérez-Rodríguez, P., Burgueño, J., Pérez-Elizalde, S., Rodrigues, F., & Toledo, F. (2023). Bayesian modelling of phosphorus content in wheat grain using hyperspectral reflectance data. *Plant Methods, 19*(1), 1–11.
Pagani, M. A., Marti, A., & Bottega, G. (2014). Wheat milling and flour quality evaluation. *Bakery Products Science and Technology*, 17–53.
Pasha, I., Anjum, F. M., & Morris, C. F. (2010). Grain hardness: A major determinant of wheat quality. *Food Science and Technology International, 16*(6), 511–522.
Pastor, K., Ačanski, M., & Vujić, D. (2019). A review of adulteration versus authentication of flour. Flour and breads and their fortification in health and disease prevention, 21-35.
Păucean, A., Mureșan, V., Maria-Man, S., Chiș, M. S., Mureșan, A. E., Șerban, L. R., & Muste, S. (2021). Metabolomics as a tool to elucidate the sensory, nutritional and safety quality of wheat bread—A review. *International Journal of Molecular Sciences, 22*(16), 8945.
Posner, E. S. (2000). Wheat. In *Handbook of Cereal Science and Technology, Revised and Expanded* (pp. 1–29). CRC Press.
Que, H., Zhao, X., Sun, X., Zhu, Q., & Huang, M. (2023). Identification of wheat kernel varieties based on hyperspectral imaging technology and grouped convolutional neural network with feature intervals. *Infrared Physics & Technology, 131*, Article 104653.
Rachon, L., & Szumilo, G. (2009). Yield of winter durum wheat (*Triticum durum* Desf.) lines in condition of different protection level of plants. *Acta Scientiarum Polonorum. Agricultura, 8*(3), 15–22.
Ran, R., Wang, C., Han, Z., Wu, A., Zhang, D., & Shi, J. (2013). Determination of deoxynivalenol (DON) and its derivatives: Current status of analytical methods. *Food Control, 34*(1), 138–148.
Razzaq, A., Guul, W., Khan, M. S., & Saleem, F. (2021). Metabolomics: A powerful tool to study the complexity of wheat metabolome. *Protein and Peptide Letters, 28*(8), 878–895.
Ropelewska, E., & Zapotoczny, P. (2018). Classification of Fusarium-infected and healthy wheat kernels based on features from hyperspectral images and flatbed scanner images: A comparative analysis. *European Food Research and Technology, 244*, 1453–1462.
Sabanci, K., Kayabasi, A., & Toktas, A. (2017). Computer vision-based method for classification of wheat grains using artificial neural network. *Journal of the Science of Food and Agriculture, 97*(8), 2588–2593.
Saia, S., Fragasso, M., De Vita, P., & Beleggia, R. (2019). Metabolomics provides valuable insight for the study of durum wheat: A review. *Journal of Agricultural and Food Chemistry, 67*(11), 3069–3085.
Salgó, A., & Gergely, S. (2012). Analysis of wheat grain development using NIR spectroscopy. *Journal of Cereal Science, 56*(1), 31–38.
Schuster, C., Huen, J., & Scherf, K. A. (2023). Comprehensive study on gluten composition and baking quality of winter wheat. *Cereal Chemistry, 100*(1), 142–155.
Shao, Y., Gao, C., Xuan, G., Gao, X., Chen, Y., & Hu, Z. (2020). Determination of damaged wheat kernels with hyperspectral imaging analysis. *International Journal of Agricultural and Biological Engineering, 13*(5), 194–198.
Sharma, A., Singh, T., & Garg, N. (2022). Combining near-infrared hyperspectral imaging and ANN for varietal classification of wheat seeds. In *2022 Third International Conference on Intelligent Computing Instrumentation and Control Technologies (ICICICT)* (pp. 1103–1108). IEEE.
Shen, G., Cao, Y., Yin, X., Dong, F., Xu, J., Shi, J., & Lee, Y. W. (2022). Rapid and nondestructive quantification of deoxynivalenol in individual wheat kernels using near-infrared hyperspectral imaging and chemometrics. *Food Control, 131*, Article 108420.
Shewry, P. R., & Hey, S. J. (2015). The contribution of wheat to human diet and health. *Food and Energy Security, 4*(3), 178–202.
Shi, Y., Liu, W., Zhao, P., Liu, C., & Zheng, L. (2020). Rapid and nondestructive determination of deoxynivalenol (DON) content in wheat using multispectral imaging (MSI) technology with chemometric methods. *Analytical Methods, 12*(26), 3390–3396.
Siesler, H. W., Kawata, S., Heise, H. M., & Ozaki, Y. (Eds.). (2008). *Near-infrared spectroscopy: Principles, instruments, applications*. John Wiley & Sons.
Singh, C. B., Jayas, D. S., Paliwal, J., & White, N. D. G. (2009). Detection of sprouted and midge-damaged wheat kernels using near-infrared hyperspectral imaging. *Cereal Chemistry, 86*, 256–260.
Singh, S., & Sharma, D. K. (2021). Deterioration of grain quality of wheat by rice weevil, Sitophilus oryzae L. during storage. *Indian Journal of Agricultural Research, 1*, 6.
Sivakumar, C., Findlay, C. R. J., Karunakaran, C., & Paliwal, J. (2023). Non-destructive characterization of pulse flours—A review. *Comprehensive Reviews in Food Science and Food Safety, 22*(3), 1613–1632.
Šramková, Z., Gregová, E., & Šturdík, E. (2009). Chemical composition and nutritional quality of wheat grain. *Acta chimica slovaca, 2*(1), 115–138.
Sun, Y., Ye, Z., Zhong, M., Wei, K., Shen, F., Li, G., & Xing, C. (2023). Rapid and nondestructive method for identification of molds growth time in wheat grains based

on hyperspectral imaging technology and chemometrics. *Infrared Physics & Technology, 128*, Article 104532.
Tahmasbian, I., Morgan, N. K., Hosseini Bai, S., Dunlop, M. W., & Moss, A. F. (2021). Comparison of hyperspectral imaging and near-infrared spectroscopy to determine nitrogen and carbon concentrations in wheat. *Remote Sensing, 13*(6), Article 1128.
Tang, H., Song, Y., Guo, J., Wang, J., Zhang, L., Niu, N., & Zhao, H. (2018). Physiological and metabolome changes during anther development in wheat (*Triticum aestivum* L.). *Plant Physiology and Biochemistry, 132*, 18–32.
Tripathi, A. K. (2018). Pests of stored grains. *Pests and their Management*, 311–359.
Troccoli, A., Borrelli, G. M., De Vita, P., Fares, C., & Di Fonzo, N. (2000). Mini review: Durum wheat quality: A multidisciplinary concept. *Journal of Cereal Science, 32*(2), 99–113.
Tyagi, N., Raman, B., & Garg, N. M. (2022). Varietal classification of wheat seeds using hyperspectral imaging technique and machine learning models. In *International conference on computer vision and image processing* (pp. 253–266). Cham: Springer Nature Switzerland.
Uthayakumaran, S., & Wrigley, C. (2017). Wheat: Grain-quality characteristics and management of quality requirements. In C. Wrigley, I. Batey, & D. Miskelly (Eds.), *Cereal grains* (2nd Edition, pp. 91–134). Woodhead Publishing.
Van Der Fels-Klerx, H. J., Klemsdal, S., Hietaniemi, V., Lindblad, M., Ioannou-Kakouri, E., & Van Asselt, E. D. (2012). Mycotoxin contamination of cereal grain commodities in relation to climate in North West Europe. *Food Additives & Contaminants: Part A, 29*(10), 1581–1592.
Varzakas, T. (2016). Quality and safety aspects of cereals (wheat) and their products. *Critical Reviews in Food Science and Nutrition, 56*(15), 2495–2510.
Vatter, T., Gracia-Romero, A., Kefauver, S. C., Nieto-Taladriz, M. T., Aparicio, N., & Araus, J. L. (2022). Preharvest phenotypic prediction of grain quality and yield of durum wheat using multispectral imaging. *The Plant Journal, 109*(6), 1507–1518.
Vermeulen, P., Suman, M., Pierna, J. A. F., & Baeten, V. (2018). Discrimination between durum and common wheat kernels using near infrared hyperspectral imaging. *Journal of Cereal Science, 84*, 74–82.
Wang, B., Sun, J., Xia, L., Liu, J., Wang, Z., Li, P., & Sun, X. (2023). The applications of hyperspectral imaging technology for agricultural products quality analysis: A review. *Food Reviews International, 39*(2), 1043–1062.
Wang, K., & Fu, B. X. (2020). Inter-Relationships between test weight, thousand kernel weight, kernel size distribution and their effects on Durum wheat milling, semolina composition and pasta processing quality. *Foods, 9*, Article 1308.
Wang, Y., Zhang, C., Wang, J., & Knopp, D. (2022). Recent progress in rapid determination of mycotoxins based on emerging biorecognition molecules: A review. *Toxins, 14*(2), Article 73.
Welch, R. M., & Graham, R. D. (2004). Breeding for micronutrients in staple food crops from a human nutrition perspective. *Journal of Experimental Botany, 55*(396), 353–364.
Wieser, H., Koehler, P., & Scherf, K. A. (2023). Chemistry of wheat gluten proteins: Qualitative composition. *Cereal Chemistry, 100*(1), 23–35.
Wu, Y., Yun, Y., Chen, J., & Liu, D. (2021). Discrimination of waxy wheats using near-infrared hyperspectral spectroscopy. *Food Analytical Methods, 14*, 1704–1713.
Yuen, G. Y., & Schoneweis, S. D. (2007). Strategies for managing Fusarium head blight and deoxynivalenol accumulation in wheat. *International Journal of Food Microbiology, 119*(1–2), 126–130.
Zhang, D., Chen, G., Zhang, H., Jin, N., Gu, C., Weng, S., & Chen, Y. (2020). Integration of spectroscopy and image for identifying fusarium damage in wheat kernels. *Spectrochimica Acta Part A: Molecular and Biomolecular Spectroscopy, 236*, Article 118344.
Zhang, G., Chen, R. Y., Shao, M., Bai, G., & Seabourn, B. W. (2021). Genetic analysis of end-use quality traits in wheat. *Crop Science*, 1709–1723.
Zhang, H., Hou, Q., Luo, B., Tu, K., Zhao, C., & Sun, Q. (2022). Detection of seed purity of hybrid wheat using reflectance and transmittance hyperspectral imaging technology. *Frontiers in Plant Science, 13*, Article 1015891.
Zhang, J., Guo, Z., Ren, Z., Wang, S., Yue, M., Zhang, S., Yin, X., Gong, K., & Ma, C. (2023). Rapid determination of protein, starch and moisture content in wheat flour by near-infrared hyperspectral imaging. *Journal of Food Composition and Analysis, 117*, Article 105134.
Zhang, L., & Ji, H. (2019). Identification of wheat grain in different states based on hyperspectral imaging technology. *Spectroscopy Letters, 52*(6), 356–366.
Zhang, L., Sun, H., Li, H., Rao, Z., & Ji, H. (2021). Identification of rice-weevil (Sitophilus oryzae L.) damaged wheat kernels using multi-angle NIR hyperspectral data. *Journal of Cereal Science, 101*, Article 103313.
Zhang, L., Sun, H., Rao, Z., & Ji, H. (2020). Non-destructive identification of slightly sprouted wheat kernels using hyperspectral data on both sides of wheat kernels. *Biosystems Engineering, 200*, 188–199.
Zhang, S., Liu, S., Shen, L., Chen, S., He, L., & Liu, A. (2022). Application of near-infrared spectroscopy for the nondestructive analysis of wheat flour: A review. *Current Research in Food Science, 5*, 1305–1312.
Zhang, S. B., Lv, Y. Y., Wang, Y. L., Jia, F., Wang, J. S., & Hu, Y. S. (2017). Physiochemical changes in wheat of different hardnesses during storage. *Journal of Stored Products Research, 72*, 161–165.
Zhang, W., Kasun, L. C., Wang, Q. J., Zheng, Y., & Lin, Z. (2022). A review of machine learning for near-infrared spectroscopy. *Sensors, 22*(24), Article 9764.
Zhang, Y., Lu, G., Zhou, X., & Cheng, J. H. (2022). Non-destructive hyperspectral imaging for rapid determination of catalase activity and ageing visualization of wheat stored for different durations. *Molecules, 27*(24), Article 8648.
Zhao, T., Chen, M., Jiang, X., Shen, F., He, X., Fang, Y., & Hu, Q. (2020). Integration of spectra and image features of Vis/NIR hyperspectral imaging for prediction of deoxynivalenol contamination in whole wheat flour. *Infrared Physics & Technology, 109*, Article 103426.
Zhao, W., Zhao, X., Luo, B., Bai, W., Kang, K., Hou, P., & Zhang, H. (2023). Identification of wheat seed endosperm texture using hyperspectral imaging combined with an ensemble learning model. *Journal of Food Composition and Analysis, 121*, Article 105398.
Zhao, X., Que, H., Sun, X., Zhu, Q., & Huang, M. (2022). Hybrid convolutional network based on hyperspectral imaging for wheat seed varieties classification. *Infrared Physics & Technology, 125*, Article 104270.
Zhao, X., Wang, W., Ni, X., Chu, X., Li, Y. F., & Lu, C. (2019). Utilising near-infrared hyperspectral imaging to detect low-level peanut powder contamination of whole wheat flour. *Biosystems Engineering, 184*, 55–68.
Zhao, X., Wang, W., Ni, X., Chu, X., Li, Y. F., & Sun, C. (2018). Evaluation of Near-infrared hyperspectral imaging for detection of peanut and walnut powders in whole wheat flour. *Applied Sciences, 8*(7), 1076.
Zheng, L., Bao, Q., Weng, S., Tao, J., Zhang, D., Huang, L., & Zhao, J. (2022). Determination of adulteration in wheat flour using multi-grained cascade forest-related models coupled with the fusion information of hyperspectral imaging. *Spectrochimica Acta Part A: Molecular and Biomolecular Spectroscopy, 270*, Article 120813.
Zhou, L., Zhang, C., Taha, M. F., Wei, X., He, Y., Qiu, Z., & Liu, Y. (2020). Wheat kernel variety identification based on a large near-infrared spectral dataset and a novel deep learning-based feature selection method. *Frontiers in Plant Science, 11*, Article 575810.
Zhu, K., Aykas, D. P., Anderson, N., Ball, C., Plans, M., & Rodriguez-Saona, L. (2022). Nutritional quality screening of oat groats by vibrational spectroscopy using field-portable instruments. *Journal of Cereal Science, 107*, Article 103520.